High Density Exudates and Basal Meningeal Enhancement in Computed Tomography of the Head in the Diagnosis of Paediatric Tuberculous Meningitis

Dr. Savvas Andronikou

Thesis Presented for the Degree of
DOCTOR OF PHILOSOPHY
in the Department of Radiology
UNIVERSITY OF CAPE TOWN
February 2005

Abstract:

High Density Exudates and Basal Meningeal Enhancement in Computed Tomography of the Head in the Diagnosis of Paediatric Tuberculous Meningitis

Dr. Savvas Andronikou

Computerised tomography (CT) scanning of the head is widely used in making the diagnosis and detecting the complications of tuberculous meningitis (TBM) in children but the individual features are considered non-specific. Hydrocephalus is encountered most frequently, followed by basal enhancement and infarction. In this paper a new feature of hyper-density in the basal cisterns on CT scans without intravenous contrast is presented and evaluated.

Aim: To determine the diagnostic value of high-density exudates in the basal cisterns on CT of the head without contrast.

Secondly, to assess the comparative importance of basal enhancement, hydrocephalus and infarction in relation to non-contrast hyperdensity.

Method: A retrospective blinded review of CT scans of patients with culture-proven TBM was undertaken and statistically analysed in comparison to the other features. Both manual and computer-aided density thresholding systems were also developed and evaluated.

Results: Non-contrast basal cistern hyperdensity is the most specific feature for TBM on CT (specificity 100, sensitivity 46%). The most sensitive feature of TBM is basal enhancement (89%) which also has a high specificity (94%). The classical combination of hydrocephalus, infarction and basal enhancement is as specific as non-contrast hyper-density, but at 41% sensitivity is worse than non-contrast hyperdensity.

Conclusion: The presence of high density within the basal cisterns on non-contrast CT scanning is a very specific sign for TBM in children, with moderate sensitivity. Use of this sign should enhance diagnostic confidence and allow earlier treatment, together with savings on contrast material, scanning time and radiation exposure. Basal enhancement offers supporting evidence. The thresholding techniques appear useful and may be applicable in other areas.

Contents:

Introduction and Background:

Tuberculous meningitis (TBM) is a serious health problem in both the developing and developed worlds [1-6]. It is the most severe life-threatening form of tuberculosis (TB) [5,7-10] and it carries a high morbidity and mortality in untreated cases, particularly in children, who are also at high-risk for acquiring the disease. TBM is also the commonest form of bacterial meningitis in children less than 13 years of age in South Africa [11]. Despite many technological advances and diagnostic tests, making the diagnosis of TBM remains demanding. The definitive diagnosis of TBM is currently made by culture of the tuberculous organism or identification of acid-fast bacilli (AFB's) on CSF smears. The yield of these tests is low and cultures are time-consuming, especially considering that delay in diagnosis and institution of appropriate therapy are the most important determinants of negative (poor) outcome. Other tests such as tuberculin skin testing and chest X-ray are neither sensitive nor specific for the diagnosis of all types of TB.

Computed tomography (CT) of the brain may suggest the diagnosis when the classically reported findings of TBM are detected. These include hydrocephalus, which is often considered to be of both diagnostic and therapeutic importance, but it is in reality a non-specific finding which may be the result of many other processes. The CT finding of basal exudates with granulation tissue has been described, but no studies aimed at identifying the value of detection of the exudate itself have been encountered. Instead, the detection of basal enhancement on iodinated contrast medium-enhanced CT has been emphasized. Very little attention has been paid to the role of CT without contrast as a diagnostic tool in TBM.

This thesis aims to investigate the postulate that non-contrast CT studies are indeed useful in making a specific diagnosis of TBM by demonstrating hyperdensity in the basal cisterns. A visual method of density-threshold to determine cistern hyperdensity is explored, as is the possibility that this may lead to an automated method of diagnosing TBM. It also aims to seek objective parameters to evaluate post-contrast basal enhancement The diagnostic CT features of TBM, specifically high density exudates,

basal enhancement, hydrocephalus and infarction are statistically evaluated in an attempt to validate the most sensitive and predictive markers of TBM. The impact of these features on earlier institution of therapy and improved clinical outcome is also examined.

Epidemiology and Demographics:

Nearly a third of the world's population are presently infected by the mycobacterium tuberculosis bacillus [1,10,12]. An estimated eight million people worldwide develop active disease annually [1,10,12]. Ninety five percent of these cases occur in developing countries with only 5% arising in industrialized countries [12]. Between 3 and 5 million people die per annum as a result of TB, with only approximately 40 000 (0.8-1.3% of the total) of these deaths occurring in industrialized countries [12]. TB causes more deaths than any other single pathogen in the world [12]. The largest numbers of people affected are from the Western Pacific, South East Asia and Africa [12], with the highest incidence in Africa (272/100 000 population). In South Africa, TB is endemic. South Africa is eighth in the list of high burden countries but has the third highest rate of smear-positive cases (194/100 000 in 2001 [13] and 214/100 000 in 2000) according to the World Health Organisation (WHO). The highest smear-positive rates occur in Cambodia (256/100 000) and in Zimbabwe (234/100 000).

Human Immunodeficiency Virus (HIV) infection increases the risk of TB [5]. It is estimated that 14% of the 10.2 million newly-diagnosed cases of TB worldwide in 2002 were linked to HIV infection [5]. In 10 sub-Saharan African countries, the HIV epidemic has lead increases of up to 100% in reported TB cases over the last 4 to 5 years [5].

In industrialized countries, 80% of TB-infected individuals are 50 years or older, while in developing countries 75% are less than 50 years of age [5]. According to the WHO, there are 1.3 million new cases of TB in children less than 15 years of age annually [1,5].

TB affecting the meninges of the brain (TBM) has been reported to account for 20-45% of all types of TB in children, but only 2.9-5.5% of adult TB [14]. The incidence of TBM in a given community is directly proportional to the prevalence of the disease in general [3], and is therefore common where the disease is endemic. [14]. TBM is seen more frequently in children than in adults in societies with a high incidence of TB, and more often in adults in societies where the incidence is lower [15]. TBM is therefore

predominantly a disease of infants and children [16-19]. The peak incidence of TBM is in the first 5 years of life [14,16,19]. Even though haemophilus influenza has been reported to be the commonest organism causing bacterial meningitis in children less than 5 years of age throughout most of the world, Donald et al showed in 1996 that in the Western Cape Province of South Africa, TBM was the commonest form of bacterial meningitis in children under 13 years of age [11,20], with an incidence of 8.6/100 000 population for those less than 15 years of age [11,20].

There are a number of risks for developing TBM.

These include:

-HIV infection (felt by some authors to be highest single risk factor) [1,2,12]
-Age, especially children less than 2 years [2,21]
-Low socio-economic conditions [2,3,11]
-Malnutrition [11]
-Overcrowding [11]
-Hygiene [3]
-Decline in public health services and in medical care [1]
-Drug abuse [3] and
-Immigration of people from countries with a high prevalence of TBM [1,3,22]

Adult versus Childhood TBM:

Children with TBM differ from adults with TBM in numerous ways. As mentioned above, TBM is more common in children than in adults in societies with a high incidence of TB in general [11,15]. TBM accounts for 20-45% of all types of TB in children, but only 2.9-5.9% of adult TB [14]. The reported incidence of hydrocephalus in children with TBM is 80-100%, while in adults is reported to be 12% [8]. The radiological findings on CT may be the same for children as adults, but the complications of TBM in children as seen on CT vary from adults in their frequency. Hydrocephalus and infarction are reported to occur more frequently in children than adults [11].

The Influence of HIV on TBM:

The HIV epidemic has contributed to a change in the face of TB [3]. In ten sub-Saharan African countries, the AIDS epidemic has resulted in increases of up to 100% in reported TB cases in the last 4 to 5 years [1,12]. It is estimated that 14% of the 10.2 million new cases of TB worldwide in 2002 were attributable to HIV [5]. HIV infection is thought to increase the chance of latent TB infection progressing to active TB, or to increase the probability of re-infection by reducing cell-mediated immunity [1,12]. HIV infected patients are therefore at increased risk of developing TB and presumably by association, TBM [3,13,23]. TB also appears to be more rapidly progressive in HIV positive patients [3]. This is particularly true in areas with endemic TB [23], such as South Africa, where HIV has shifted the spectrum of meningitis towards chronic infections such as TB [13]. TB is an AIDS-defining condition, and in one study 59% of patients with TBM infection also had HIV infection [23].

As the HIV infection primarily impairs cell-mediated immunity, responses to TB bacilli in HIV-infected individuals may be altered and hence the pathological features seen in HIV positive patients may differ from those with normal cell-mediated immunity. This may also be reflected in different clinical and radiological features [5]. HIV infection does not significantly alter the clinical and CSF findings of TBM in adults in South Africa [13]. Children co-infected with HIV, however, are likely to be anergic to Mantoux testing [1].

Post-mortem studies have shown that HIV positive patients with TBM have thin, minimal and/or serous exudates only in the cisterns of brain compared with more substantial pathological processes in the HIV-negative group [5]. In HIV TBM patients, the major arteries are free of exudates, there is no CSF-outflow obstruction and milliary tubercles are absent [5]. This is in contrast to HIV-negative patients, who have thick, gelatinous exudates involving the major arteries, obstructed CSF outflow leading to hydrocephalus, and milliary tubercles on the meninges [5].

On CT, HIV positive patients may show more cortical infarcts [5,13]. Ventriculomegaly is common in HIV per se [13], but is more likely representative of atrophy [24]. True communicating hydrocephalus and basal enhancement are not major features of HIV-positive patients with TBM. Basal enhancement, when present, is mild and seen only after anti-tuberculous therapy [5,13].

Pathogenesis:

TB is primarily an air-borne disease [2]. Close proximity to an infectious adult poses a risk, and transmission to children usually occurs from such an adult [2]. Infected droplets produced by coughing, sneezing or talking spread through the air and are inhaled by the child [1,2,8,25]. This transmission is felt to account for 95-98% of cases of childhood TB [1,25]. Rarely an infant may acquire TB congenitally, either through the placenta or via infected amniotic fluid [2]. Children seldom infect each other, as children with pulmonary TB rarely cough, and if they do, seldom produce sputum. Furthermore, the lesions of primary TB are not heavily laden with tubercle bacilli, as opposed to the cavitatory lesions of secondary TB in adults [25].

The two factors that most determine the chance that TB will develop are environmental (the likelihood of exposure to another person with infectious TB) and host-related (the ability of the individual's immune system to control the infection) [1].

Once inhaled, the TB bacillus travels to the lungs and begins to multiply in the lung parenchyma [2]. Tubercle bacilli then enter and spread via the lympho-haematogenous route [8] to other organs [2]. Bacilli reach the central nervous system via the haematogenous route [3,8,11,18,19,21,25-27]. This usually occurs within 2 to 6 months of primary lung infection [11,25]. Small TB lesions (Rich foci) develop in the central nervous system during the bacteraemic phase [3,11,21,26]. The initial lesion may be in the meninges, brain or spinal cord [3], and can become active after a quiescent period, which may be years after the initial infection [3]. TBM is believed to be the result of CSF seeding following rupture of pial or sub-pial granulomata into the subarachnoid space [3,11,21,26-28]. The resultant disease has a basal predominance, but the reason for this is not known. The intense inflammatory meningeal reaction that results is thought to be due either to the direct effect of the TB bacilli, or an allergic response to the tubercle protein [27]. Meningeal involvement by TB may also rarely occur from adjacent TB infection, such as sinusitis or osteomyelitis [27].

Pathology:

Established TBM is characterized by a granulomatous inflammatory reaction involving the leptomeninges throughout the subarachnoid space, particularly at the base of the brain [14,15], sometimes erroneously termed a fibrinous pachymeningitis [19]. The inflammatory response may be due to the direct effects of the TB bacilli, but most authors believe that it is a hypersensitivity response to the tuberculoprotein [21,27]. The inflammatory reaction is characteristically both necrotising and proliferative resulting in vasculitis, infarction and hydrocephalus with resultant increased intracranial pressure [24,29]. There may also be concurrent granuloma formation [24].

The Exudate

In patients dying from TBM the basal meninges and cisterns are typically obscured by a thick, grey, gelatinous exudate within which miliary sized tubercles are often apparent. In some cases, confluent granulomata constitute the reaction, and in others, the exudate is strikingly asymmetrical, affecting one Sylvian cistern and fissure [3,14,16,21,26,27,30-34]. Patients dying during the course of anti-tuberculous therapy, display leptomeningeal fibrosis with adhesions surrounding the basal vessels, optic chiasm and infundibulum, and characteristic loculation of the subarachnoid space, most prominent in relation to the outlet foramina [personal communication Prof Richard Hewlett].

Tuberculous granulomatous arachnoiditis is usually inferred by the presence of abnormal basal enhancement on CT scanning and by the complications of infarction and hydrocephalus. The detection of exudates on CT without intravenous contrast has only been mentioned in two publications [3,26].

Tuberculous Encephalopathy

Ischaemic injury and CSF obstruction comprise the principal pathogenetic processes leading to parenchymal damage [3,14,17,21,26-28,30,34-40].

Vasculopathy and ischaemia:

Pathomorphology includes a spectrum of inflammation, necrosis and occlusion often in combination, although not exclusively. In particular, intimal proliferation with occlusion constitutes the so-called 'obliterative endarteritis' of Heubner. Examination of the fixed brains of individuals with advanced TBM frequently reveals widespread basal infarction [personal communication Prof. Richard Hewlett]. These changes, especially vascular necrosis, are all assumed to be part of the hypersensitivity reaction whilst rarely there may be direct involvement of the vessel wall by a necrotising granuloma. Cerebral infarction is a common complication of TBM [38,39], with reported incidences from 6-41% [18,38,39]. Most frequently affected vessels correspond with the locations and severity of the inflammatory response [28,39], including the terminal portions of the internal carotid artery [15,26,27,39], M1 segment of the middle cerebral artery [3,15,17,21,26,27,39] and their perforating branches [3,15,21,26,39] (especially the lenticulostriate branches) [39,40] as well as the Sylvian branches of the middle cerebral artery [15,16,39]. Infarcts are therefore most frequently seen in the basal ganglia, hypothalami, thalami and internal capsules [3,15,17,28,32,38,40] as well as the middle cerebral artery territory [15,17] and either side of the Sylvian fissures [15]. The vertebrobasilar vessels are less commonly affected [35,39]. Infarcts in the other major vascular territories or brainstem are rare [38,39].

Encephalopathy

TBM is properly a meningoencephalitis, with associated superficial parenchymal inflammation including focal necrotising granulomata, ischaemic and toxic neuronopathy, coagulative pan-necrosis, oedema and astrocytosis [personal communication Prof. Richard Hewlett]. Non-ischaemic neuronal shrinkage has been referred to as the border-zone reaction [35] and may be apoptotic. It is not uncommon to find genuine pyogenic microabscess formation as part of TB encephalopathy [16],

combined with the predominant granulomatous response. However, significant loculation is always due to necrotic macrophages, and is properly defined as pseudo-abscess formation. Perivascular demyelination has been proposed to occur as an allergic hypersensitivity reaction [35,36] (though not seen in the Cape Town material) [personal communication Prof. Richard Hewlett].

Tuberculous Granuloma:

The TB granuloma may be microscopic or macroscopic, may form in any part of the brain parenchyma, subarachnoid space or dura, and is invariably necrotising to a degree. Necrosis in most lesions is gummatous (coagulative), though often with a liquefactive (caseous) component. Gummatous granulomata exhibit florid macrophage-epitheloid cell formation, with encapsulation by inflammatory granulation tissue, and usually lack easily demonstrable bacilli. Less commonly the tuberculoma is wholly liquefactive (TB pseudoabscess) and may form very large extraparenchymal loculi, sometimes within the subdural space [personal communication Prof Richard Hewlett]. The relationship of tuberculoma pathomorphology histopathology to the evolution of TBM is unclear. Tuberculomata can occasionally be associated with mass effects [35].

Hydrocephalus

The pathogenesis of hydrocephalus in TBM includes the effects of the exudates within the subarachnoid space, particularly the proliferative component, and with regression, residual leptomeningeal fibrosis [3,7,11,14-16,21,22,26,27,29,33,35,36,41,42].
Both mechanisms result in communicating hydrocephalus [3,7,11,14,21,27,29,41,42,43], the commonest type of hydrocephalus in TBM [11,21,29,33,40,41].
Non-communicating hydrocephalus [3,14,21,27,29,35,41,42] is usually the result of choroid plexus-leptomeningeal fibrosis at the level of the lateral foramina [personal communication Prof. Richard Hewlett] [3,14,15,27,29,33,36,42].
Obliteration of the CSF space constituting the ambient cistern may lead to a distinctive form of 'intermediate level' block, with dilation of the posterior fossa cisterns [personal

communication Prof. Richard Hewlett]. Obstruction due to a mass lesion is rarely seen [21,35,41].

Morbidity and Mortality: Necessity for Early Diagnosis and Treatment

TBM is the most lethal form of tuberculosis in infants and children [8]. Untreated TBM is almost invariably fatal within a few weeks [14,27]. Reported overall mortality rates on treatment vary between 15 and 60% [4,7,41]. It is estimated that 170,000 children die annually as a result of TBM [44]. It also has a high morbidity [1,3,9,10,36,38,40,41,45], with major cost and personal implications. In India TBM accounts for up to 9% of paediatric hospital admissions [46].

TBM is a potentially treatable disease that responds to specific anti-tuberculous medication when commenced early. The most important prognostic factor determining poor outcome is the delay between the onset of symptoms and initiation of anti-tuberculous therapy [4,16,17,21,38,43]. The high morbidity, mortality and potential for rapid deterioration or decompensation associated with TBM therefore require an early diagnosis to be made [3,7-9,41,45,46], with rapid commencement of aggressive treatment [3,7,9,45,46].

Clinical Presentation:

The clinical presentation of TBM reflects the evolving basilar fibrinous pachymeningitis and vasculitis [19], with subsequent parenchymal damage and raised intracranial pressure [40,47]. The onset of symptoms may be insidious, especially in children [7,13,16,41,45], but can have an acute onset in up to 50% of affected cases [16,41]. Symptoms are frequently non-specific, especially in the neonatal period [7,16,41], and may be confused with those of other infantile infectious diseases [7,16].

Classical findings of early TBM include:

-Mild fever [41,45]
-Apathy
-Unwillingness to play [16,41]
-Irritability [41]
-Headache [1,45,48]
-Loss of appetite [1,16]
-Nausea [41,45]
-Vomiting [41,45]
-Abdominal pain [41]
-Stiff neck [45]
-Lethargy [16]
-Weight loss [16]

The patient then deteriorates to present with more evident symptoms such as:

-Features of raised intracranial pressure [16,27]
-Extreme lethargy [16]
-Moderate fever [16]
-Nuchal rigidity [16,48]
-Cranial nerve palsies [16,27]

-Convulsions [9,16,48,49]

-Coma [16]

-Decerebrate status [16]

-Hemiplegia [37]

- Syndrome of inappropriate anti-diuretic hormone (SIADH) secretion [49]

Many cases may have an onset without symptoms, with the diagnosis only being made when the patient deteriorates [2,45].

Many authors promote the United Kingdom Medical Research Council staging system devised in 1948 to classify the severity of patients on admission [11,28,32,34,40]:

Stage I: Fully conscious without paresis or focal neurological signs

Non-specific signs and symptoms

Stage II: Drowsy or decreased level of consciousness (but localizing pain and/or mild focal signs)

Stage III: Deeply comatose with or without gross paresis

[11,28,40]

In most studies from developing countries, patients present in stages II or III. This is in contrast to the typically less severe illness on presentation in industrialised countries [50].

Diagnosis:

Diagnosis – general:

A specific diagnosis of TBM is conclusively established by isolation of acid-fast bacilli on cerebrospinal fluid smears using Ziehl-Nielsen or auramine/phenol stains or by the demonstration of the mycobacterium tuberculosis bacillus on cerebrospinal fluid culture or guinea pig inoculation. These laboratory tests remain the 'gold-standard' for making the diagnosis [45].

Caseous necrosis on histopathological specimens is also considered almost conclusive of the disease [18,26,45].

Secondary suggestive criteria in making the diagnosis of TBM in the absence of a positive culture or smear are covered in more detail below but include:

-History of exposure to an adult with active TB [21,51]
-Positive Mantoux test
-Evidence of TB in another site in the body [21] e.g. a suggestive chest radiograph [51]
-Cerebrospinal fluid changes compatible with TBM [26]
-No evidence of any other aetiology [51]
-As a last resort, a therapeutic trial of response to specific therapy [26,51]

Negative TB culture, negative Mantoux, a normal ESR and previous BCG vaccination do not exclude the disease [3].

Newer diagnostic tests such as enzyme linked immunosorbent assay (ELISA), bromide partition test, a test for tuberculo-stearic acid in the CSF and polymerase chain reaction (PCR) detection of TB DNA are unlikely to be available in many countries for some time [9].

Diagnostic Criteria:

The formal diagnostic criteria for TBM are not well established [10], and vary considerably in the reported series [5,7,13,15,28,39,43,45]. Several authors categorize their patients into groups such as:

Definite

Highly probable

Probable and

Possible,

using different combinations of diagnostic criteria.

Definitive diagnosis by CSF culture or identification of acid fast bacilli on stained smears of CSF is universally accepted, but even culture or smear-positivity from other body fluids such as gastric aspirates or sputum have been used as proof of TBM.

The other diagnostic criteria used include clinical findings (especially a close contact history), CSF profile, extra-neurological evidence of TB, Mantoux positivity, chest radiograph findings, response to anti-tuberculous therapy and even a negative bacterial culture for organisms other than TB [4-10,29,37,38,40,41,45-47,50,52,53]. Others include the CT findings felt to be characteristic of TBM [6,11,24,45,50].

Diagnostic Difficulty:

The diagnosis of TBM is difficult to make, especially in the paediatric patient [2,9,10,13,16,34,46] during the early stage of the disease [17]. Diagnostic confusion exists between TBM and other meningoencephalitides [9]. Partially treated pyogenic meningitis, in particular, may be indistinguishable at presentation [9,46]. Antibiotics prolong the course of pyogenic meningitis and alter the CSF profile [9]. TBM may also be inseparable from cryptococcal meningitis as they share many clinical and CSF features [38]. Lack of familiarity with TBM, especially in areas of low incidence, may contribute to the delay in diagnosis [17,21]. The presence of focal signs may delay the performance of a lumbar puncture, for fear of inducing transtentorial herniation [28,34].

Culture of tubercle bacilli from CSF using traditional methods takes 4 to 6 weeks [9,17,28,45,51] and has a low yield [9,45,46,54]. The BACTEC method, which is used in

our institution yields better results in a shorter time, but nonetheless takes from 7 to 10 days to show organism growth [51]. Identification of AFB's on Ziehl-Nielsen stains from CSF is rarely positive [9,17,21,34,54], and pickup rates decrease after the first five days [41].

Therefore, bacterial proof of TBM is only available in a small proportion of patients [9] and the initial diagnosis of TB often has to be made on supportive evidence [54]. Whereas TB bacilli may be regularly found in the sputum of older children and adolescents, young children do not produce sputum and cultures are difficult to obtain in this age group [2,51]. Gastric aspirates are the alternative to sputum culture, but only 30-40% of these yield organisms [51] and once again culture may take several weeks [2]. Mantoux tests are also problematic in making an early diagnosis. They can only be read 48-72 hours after administration, and a negative Mantoux test occurs with sufficient frequency in all forms of active TB that it is of little help in excluding the disease [21]. The causes of false negative results in children are listed below in the Mantoux section. Chest radiographs may not show any abnormality in TBM and are also fraught with problems in the detection of lymphadenopathy, the hallmark of primary TB. Blood tests are often entirely normal [21].

Most of the newer tests are unlikely to be widely available in the near future [46]. A diagnosis made by assessing the response to treatment is time-consuming and could lead to incorrect treatment [45,46]. The CT features of TBM are available immediately, but are regarded by some as non-specific at present [17,27]. The motivation for this research project is to determine any specific CT features of TBM with a high positive predictive value.

CSF Culture:

CSF culture has a variable yield [4,5,54], ranging from 5 to 87% [4,5,8]. Repeated CSF cultures increase the positivity to 52-83% [41]. Negative culture does not rule out the disease [1,15]. Culture may take several weeks to become positive because of the slow growth of mycobacterium tuberculosis [7,15]. Traditional methods of culture involve the Lowenstein-Jensen and Middlebrook media (both solid media) and it is these methods

that require 4-6 weeks for organism isolation and a further 2-4 weeks for antibiotic sensitivity testing [1]. At our institution the 'BACTEC' radiometric system is used. This is a liquid medium, which yields culture and susceptibility results in as few as 7-10 days, and is also more sensitive than other methods of TB culture [1].

CSF Staining

Isolation of AFB in CSF using Ziehl-Nielsen or auramine/phenol staining also has a low yield [5,54], ranging from 10 to 87% [8,29]. Repeat smears lead to 39-87% detection rates. Smear sensitivity relative to culture may vary from 50-80% [55].

Cerebrospinal Fluid Profile:

Laboratory evaluation of CSF is often the key to suspected diagnosis clinically, prior to receiving culture results. The CSF levels of white blood cells, lymphocytes, protein and glucose, and the CSF-to-blood glucose ratios are variable in TBM [4], but a CSF profile that is very suggestive of TBM would constitute:

-Lymphocytic pleocytosis

-Elevated protein concentration

-Reduced glucose level (both absolute and relative to blood glucose)

-Elevated CSF pressure and

-Elevated adenosine deaminase (ADA) levels [3,13,21,25,34,41,45].

However, exceptions to the above are often seen [13], particularly in the first stage of the disease where there may be a polymorphonuclear predominance with borderline protein and glucose levels [25] Occasionally CSF may be completely normal [45]. The CSF profile is also often altered by commencement of empiric antibiotic therapy.

Mantoux Testing:

The Mantoux tuberculin skin test (also referred to as the purified protein derivative (PPD) test) is the chief diagnostic tool for evidence of exposure to tuberculous [1,2,51].

An intradermal injection of PPD is given, and the result is read 48 to 72 hours after being performed [2], which may delay treatment. The cut-off size for a positive reaction varies

with the person tested and epidemiological factors, but the generally applied ranges vary from 5mm to 15mm [1,51]. A 15mm cut-off is used at our institution. A negative Mantoux test never excludes TB infection or disease in a child [1].

Numerous factors in the general population and the individual can affect the Mantoux test [1,51]. The higher the prevalence of TB in the population, the higher the positive predictive value of the test [1] (as predicted by Bayes Theorem).

Causes of false positive reactions include:

-Infection with non-tuberculous mycobacteria [1,51]
-Bacille Calmette-Guerrin (BCG) vaccination up to 10 days prior to administration of the Mantoux test [1,51]

False negative reactions can occur as a result of anergy, for example in overwhelming disease, including tuberculosis, or having inadequately developed cellular immunity [2], especially in the very young [1].

Specific causes of false negative results include:
-Impaired T-cell function, as in HIV infection
-Viral illness
-Neoplastic disease
-Immunosuppressive therapy
-Malnutrition
-Live virus measles vaccination
-Early testing prior to development of a hypersensitivity reaction [1,51].

Buttaro et al report that only 90 to 95% of children with culture-positive TB of all types have a positive Mantoux [2], while Waeker et al report that less than 50% of patients with central nervous system TB have a positive Mantoux test [7].

TB Contact:

Searching for the presence of TB in the adult family or in close contacts is the most important epidemiological feature strongly suggesting the disease [4], but this may be difficult to establish for the clinician.

Sputum:

A search for AFBs on stained sputum smears is the most rapid and specific method for detection of mycobacteria in adults [56]. However, sputa are seldom available from children as they rarely cough with pulmonary TB and when they do, this is seldom productive [2,51]. It is estimated that 5×10^3 to 1×10^4 AFB per millilitre of sputum must typically be present to be detectable on microscopy, which explains the low sensitivity [56].

Gastric Aspirates:

This is an alternative to sputum testing that relies on swallowed sputum. It should be obtained in younger children [51]. Unfortunately the yield of cultures of early morning gastric aspirates from children with pulmonary TB is at best 40% and the time delay required for the culture may delay therapy [1].

Chest Radiographs:

Some patients with central nervous system TB have a positive chest radiograph, but many do not [7]. In general, an infected child with any radiographic manifestation consistent with TB is considered to have the disease, even if no symptoms are present [1]. Up to 43% of children less than 1 year of age with untreated TB infection will have chest radiographic evidence of disease, but this decreases to 24% in children aged 1 to 5 years and to 15% in adolescents 11 to 15 years of age [1].

Response to Treatment:

A therapeutic trial with clinical follow-up and evaluation of response to treatment often has to substitute as the diagnostic 'gold standard', and is a valuable tool for retrospective diagnosis [9].

Serodiagnosis:

Enzyme linked immunosorbent assay (ELISA) has been used to detect antibodies to various purified or complex antigens of mycobacterium tuberculosis in children [57,58]. Numerous commercially available kits make use of immunochromatographic strips for this [58]. Although one study reported a very high sensitivity and specificity for serum testing [1], a more recent study has shown only 26% sensitivity and 40% specificity for diagnosing TB in children [57]. It is therefore unlikely that this test will make a substantial contribution to diagnosing TB in children.

DNA Probes:

A promising method of rapid diagnosis using DNA probes complementary to specific RNA or DNA sequences of mycobacterium TB has been described recently. Radio-labelled DNA is hybridised with specimens containing suspected mycobacterial nucleic acids and the result is measured using a gamma counter. Sensitivity and specificity of commercially available techniques approach 100% in the laboratory [1], but this technique has yet to have a clinical impact.

Polymerase Chain Reaction:

DNA amplification by polymerase chain reaction (PCR) to demonstrate the DNA of TB in CSF has been used for TBM [8,56], and is claimed to be potentially the method of choice in the future by overcoming the limited sensitivities of smear examination and the delayed results of culture [56]. This technique involves first isolating the specimen containing suspected mycobacterial DNA and then amplifying it by 10^5 copies by means of DNA polymerase chain reaction using thermal cycling. Primers determine the DNA sequences targeted for amplification, and the amplified DNA is detected either by nucleic acid probes or special electrophoresis gels. Results are available in 72 hours [1]. Despite its dramatic in vitro scientific value, PCR is in practice not as sensitive and specific as expected for the detection of mycobacterium TB in clinical specimens [56]. Reported sensitivities range from 33% to 90% and specificities from 74% to 100% [8,56].

It is possible that the PCR technique will be too sensitive for use in children, especially in endemic areas [1]. In most children with either asymptomatic infection or recent TB infection, it may be possible to detect the presence of mycobacterial DNA. Detection of TB DNA does not distinguish between infection and disease [1]. Different laboratories report false positive PCR rates that average 7% [56]. These tests are unlikely to be available where they are really needed for at least the next decade [5,8,9] due to the high costs involved [5]. The practical value of PCR for early diagnosis of TBM in children at this stage is therefore very limited [8,56].

Computed Tomography (CT):

CT is well established as an effective method for the detection and localization of intracranial lesions [37], and has both high diagnostic sensitivity and accuracy in general [33]. The role of CT in the diagnosis of intracranial TB, including TBM, has been well described [21,22,26,30,32,40,50,59]. CT should be performed as an initial diagnostic test in children suspected of central nervous system TB [7,33,43] as the preferred radiological technique [43]. Some authors believe that an entirely normal CT scan in a drowsy patient excludes the diagnosis of TBM [18,28]. The performance of an early CT with resultant likely diagnosis of TBM allows for early institution of anti-TB therapy [16,28,34]. CT may be necessary prior to a diagnostic lumbar puncture when there is fear of inducing transtentorial herniation in patients with raised intracranial pressure [28]. CT is an accurate means of detecting the intracranial complications of TBM [60], including infarcts and hydrocephalus [21,47,60], and the suggestive features of TBM, including basal enhancement, exudates and tuberculomata [21,43,47]. CT also provides additional information such as prognostic information [11,26,34], differentiation from other meningoencephalitides [9,22], follow-up of hydrocephalus [21,59] and permits the monitoring of the effectiveness of treatment with steroids and ventricular drainage or shunting [21,26].

Magnetic Resonance Imaging (MRI):

The advantages of MRI over CT include lack of ionising radiation, multiplanar imaging, lack of bone artefact and good contrast resolution, especially between enhancing meninges and the low signal of bone and vessels [17, 30]. Disadvantages of MRI include poor visualization of calcification [3], difficulty in accommodating ICU-based patients because of incompatibility of standard life-support equipment with MRI and the lack of availability of MRI where it is needed most. MRI with gadolinium, however, shows basal meningeal enhancement earlier [17] and with greater sensitivity than CT. One study showed that gadolinium-enhanced MRI was generally similar to post-contrast CT in demonstrating meningeal inflammation and granulomas, but subtle inflammation of the basal cisterns was more readily depicted on MRI [30]. It is generally accepted that MRI demonstrates all the features of TBM (other than calcification) better than CT [3]. MRI easily distinguishes basal enhancement from the flow-voids of the vessels of the circle of Willis in cases where CT is equivocal for basal enhancement [30]. T2-weighted and diffusion-weighted images are sensitive for ischaemic infarcts and demonstrate them more often than CT [30,47]. MRI has also shown ischaemic lesions in the brainstem that are not visible on CT [47]. Obliteration of the ambient cisterns has been shown on T2-weighted MRI and may correlate with the exudates in the cisterns seen on CT [47].

It is unlikely that MRI will contribute significantly to the diagnosis of TBM in children in endemic areas. This is primarily due to limited access and costs, but is also restricted by the technical constraints of anaesthesia for young patients who are required to lie still for long periods, and available monitoring equipment may be incompatible with MRI.

Differential Diagnosis of TBM:

Early in the course of TBM, the clinical presentation may be similar to that of other infantile and childhood subacute or chronic infectious meningeal or cerebral diseases [7]. Clinical diagnostic confusion can exist between TBM and other meningoencephalitides [9]. The differential diagnosis of the clinical presentation of TBM includes:

pyogenic meningitis [3,16,21,46], fungal meningitis (candida / cryptococcus / coccidiodomycosis) [3,9,16,21,41], neurocysticercosis [3], neurosarcoidosis [3,21,41], meningeal carcinomatosis [3,21], viral meningoencephalitis [9,16,21], neurosyphillis [21], CNS brucellosis [21], neuroborelliosis [21], CNS toxoplasmosis [21], cerebrovascular accidents [21] and parameningeal suppurative foci (sinusitis / abscess) [21].

Bacterial meningitis may have characteristic laboratory findings, organisms may be present on smears, and cultures may be positive within 24 to 48 hours [16]. Fungal meningitis may show similar clinical and CSF features to TBM [38], but in over 90% of cases occurs in patients on immunosuppressive or long-term broad-spectrum antibiotic therapy [16].

CT Scanning:

Description:

Computed Tomography (CT) permits the examination of tissue by refining the principles of conventional X-ray imaging. Radiation passes successively through tissue from multiple different radial directions [61]. A computer correlates measurements of strength of X-rays passing through different paths and builds up a numerical cross-sectional picture based on attenuation differences. It provides an explicit image of the brain dependent on X-ray attenuation analogous to gross pathology sections of the brain seen at autopsy [62]. CT provides in-vivo information regarding the content and character of tissue comprising organs and masses [63]. It offers differential visualization of tissues with different absorption coefficients (i.e. number of X-ray photons absorbed) [64]. The fundamental advantage of CT over conventional X-ray techniques is that it can show brain and other tissue with excellent contrast resolution [62]. CT scanning is widely available, quick, costs less than MRI and standard life-support equipment is incompatible with MRI. Technical advantages include sensitive detection of calcium and haemorrhage, and excellent demonstration of the bony base of the skull. CT is also less degraded by motion than MRI, and is also very useful when MRI is contraindicated e.g. patients with aneurysm clips, foreign bodies, pacemakers or certain metal prostheses [61,63].

The history of CT and its use in children:

CT is a technique conceptualised by a South African, Cormack in the 1950's and later modified by Oldendorf in 1961. It was further developed and commercialised by Hounsfield of EMI laboratories in 1969 [63]. In October the 1971 the first patient was examined by Dr. James Ambrose, using a prototype [65]. Clinical results were made public at the annual congress of the British Institute of Radiology on April 19, 1972 by Ambrose [66]. In 1975 the absorption coefficients of any material (on an arbitrary scale) were named 'Hounsfield Units' (HU) [65]. Also in 1975, a Southern Rhodesian Harwood-Nash and Houser published the first papers of specific use of CT in children [64,67]. Harwood-Nash et al noted that CT clearly demonstrated the outlines of the ventricles and any brain calcifications. They reported that the determination of the

absorption coefficient of any area of brain was possible and that as a result, abnormalities that were neither space occupying nor vascular could also be localized [64].

Scanning technique, the machine and physics principles:

The patient lies supine on the scanner bed within the gantry. The X-ray tube and detector assembly (which are fixed in relation to each other) rotate around the axis of the patient from head to foot [62,68,69]. A fan shaped beam of X-rays penetrates the body from many angles as the X-ray tube revolves around the patient [63,65,66,68] who is moved incrementally into the gantry 'tunnel'. Original units used two detectors [66,68,69] but more modern units use multiple rows of detectors (multislice CT) to reduce scan times. A computer processes the data and reconstructs an image [66,68,69].

The body part examined is divided into a series of cubes (voxels), each having a calculable X-ray absorption [66,68].

$$\text{Absorption} = \text{Log}\ \frac{\text{Intensity of the X-ray at the source}}{\text{Intensity of the X-ray at the detector}}$$

Providing there are more X-ray readings at different angles than picture points, the absorption value of each cube can be determined [63,68] and a picture is built up as a matrix of picture points (pixels) to which numerical values (absorption coefficients) are ascribed. The final data can be manipulated and displayed on computer monitors (using variable display settings and reconstructions) and on hard copy (film). Digital storage for later retrieval and viewing is also possible [63].

An arbitrary scale of values for absorption coefficients has been set with bone and metal being the highest values, air the lowest and water as zero [63,67]. Absorption coefficient numbers are converted to specific grey scale levels [65] using a sliding scale, window width and window level system. This visual display ranges from white (dense bone or metal) to black (air) [63,64]. Controls on the display unit can be used to set sensitivity by

means of the 'window width', and to set the centre of the scale by the 'window level' [63,64,66], allowing emphasis of different characteristics of tissue in a slice [65]. The expanded Hounsfield range extends from –1000 to +1000 units. CSF normally measures in the range of 0-11 HU, white matter in the range of 12-18 HU and cortical grey matter 18-30 HU with occasional values reaching 36 HU [66].

Advantages of intravenous iodinated contrast medium in CT:

The use of intravenous iodinated contrast medium has lead to better detection of well-vascularised lesions as it results in a measurable increase in the absorption value [66,70]. This occurs because iodinated contrast media have a high atomic number and electron density, and therefore have high HU values [61,70]. Intravenous contrast media distribution reflects the integrity of the blood-brain-barrier, which is disrupted in neurologic disorders, including stroke, tumours, inflammation, infection and multiple sclerosis [61]. Extravascular spread of contrast medium is thought to occur when the blood-brain barrier is disrupted, suggesting that enhancement does not only represent increased vascularity of a lesion [70]. This is an important consideration when postulating the mechanism of basal enhancement in the cisterns in patients with TBM, where vascularised granulation tissue in the cisterns may result in cisternal enhancement, or where this may occur due to leakage of contrast out of the vessels across the blood-brain-barrier.

CT Features of TBM – General:

CT has been used as a diagnostic tool for TBM, and not only for the detection of complications [42] and follow-up. Availability of CT scanning and effective antimicrobial therapy have contributed to the better management of TBM [6]. CT scanning's wide availability with low marginal costs make it ideal for the diagnosis of TBM in the public sector where the majority of these patients present [46]. A CT scan of the head should form part of the initial assessment of any child suspected with TBM [10]. This provides baseline data and detects complications such as hydrocephalus that may require active intervention [10,18,32]. With the increased use of CT, the findings of TBM have become well recognized [28] but are reported by some authors as non-specific [17, 27]. CT scan with intravenous contrast is recommended, at a suggested dose of up to 2-ml/kg body weight [16]. Routinely 1 ml/kg body weight for head scans is used at our institution (Red Cross Children's Hospital, Cape Town) in children, with good results. The radiological features of TBM on CT reflect the pathophysiology of the disease [17]. Other than hydrocephalus, infarction (usually of the basal ganglia), co-existing tuberculomata and contrast enhancement of the basal cisterns are well seen [8,10,17,18,21,28,30,40,43,46,49,71]. Obliteration of the basal cisterns [17] and identification of gelatinous exudates have also been recorded [43]. Some authors consider the triad of basal enhancement, hydrocephalus and infarction as diagnostic of TBM [71], but most refer to these findings in combination as 'strongly suggestive' [21,40]. Numerous authors consider non-contrast CT scans to be non-diagnostic [3,40,72]. CT scans in TBM can also be completely normal, however [28].

Deviations from the normal, in general, can be visually recognized even if attenuation values are not measured directly in every particular case. Direct measurement of an area on a particular scan slice can be obtained by using an interactive region of interest (ROI) cursor with numerical density readout. This requires input to decide on the areas needing to be measured. For the most part subjective judgment is employed, which although not

scientifically rigorous is common in many medical activities [65]. Involving multiple readers in a consensus system for determining the final results may reduce reader bias.

CT scanning may demonstrate features that are common to numerous aetiological agents or, less likely, demonstrate features that strongly suggest a specific diagnosis. Other conditions that can simulate the CT features of TBM are fungal meningitis, torulosis, neurosarcoidosis and carcinomatous infiltration [9]. Viral meningoencephalitis has few characteristic CT findings [16], except for herpes necrotising encephalitis that has a propensity to affect the temporal lobes. Haemophilus meningitis (the most common pyogenic pathogen causing meningitis) often has associated subdural effusions and low densities in the anterior poles of the frontal lobes [16].

Communicating hydrocephalus on CT is not specific to TBM and can also be found in fungal, bacterial and viral infections, as well as in toxoplasmosis and subarachnoid haemorrhage [41]. The features of communicating hydrocephalus may in some cases be indistinguishable from atrophy and can also be very similar to the normal appearance of the subarachnoid space and ventricles in neonates and infants. Basal enhancement is not specific for TBM and may be seen in torulosis, neurosarcoidosis, neurosyphilis, coccidiodal meningitis, [22,46] recent subarachnoid haemorrhage, leptomeningeal carcinomatosis and lymphoma [22], but has not been reported for pyogenic meningitis [46] or viral meningoencephalitis [27].

Prognostic Value of CT:

CT has been reported to have prognostic accuracy [33], with a number of individual CT findings have been proposed to have prognostic significance, but there is variability in opinion on the values of these [4]. CT features that are reported to predict a poor outcome include hydrocephalus [4,6,14,32,42,71], periventricular lucency [34], the amount and density of exudates [33,36,71], basal enhancement [8,10,15,27,32,40,42], infarcts [6,38,39,42,71], parenchymal enhancement [42] and cerebral oedema [42].

Hydrocephalus:

Some authors report that particularly in the early stages of TBM, ventricular dilation is not necessarily indicative of a bad prognosis [32,71]. Two authors report that hydrocephalus alone carries a good prognosis [21,34]. Schoeman et al have extensively studied hydrocephalus in children in large groups of patients with TBM, and they concluded that there was no significant difference in outcome or mortality between children with large (i.e. hydrocephalus) or small ventricles on admission [40]. The same authors in a different study concluded that the poor prognosis associated with stage III TBM could not be ascribed solely to pressure hydrocephalus [47], and that neither the size of the ventricles nor the degree of raised intracranial pressure on admission correlated with prognosis [52]. No difference in outcome was found in one study between patients with communicating hydrocephalus who were shunted early compared to those who were shunted late [40], while another author showed the converse [42].

Infarcts:

Lan et al report that cerebral infarcts have a far more significant role than hydrocephalus with regard to predicting outcome [38]. Bilateral infarcts, particularly of the basal ganglia, invariably carry a poor prognosis [40]. The best outcome is when there is a normal CT scan on admission [34]. Normalisation of intracranial pressure in one study did not change the poor outcome in patients with bilateral basal ganglia infarcts [40].

Exudates:

Non-enhancing exudates are reported to have a good prognosis [27]. Numerous reports indicate that the presence of exudates (as determined by basal enhancement on post-contrast scans) are associated with a poor prognosis [8,33,36].

Primary Hypothesis: High-density cisternal exudates in CT of the brain without contrast and post-contrast basal meningeal enhancement are independently more predicative signs for the diagnosis of tuberculous meningitis in children than is hydrocephalus.

Aim: To determine the specificity, sensitivity, positive and negative predictive values and likelihood ratios of high-density exudates in the basal cisterns on non-contrast CT scanning, and of basal meningeal enhancement in the diagnosis of paediatric tuberculous meningitis and to compare them with the presence of hydrocephalus as a diagnostic test.

Materials and Methods:

A retrospective review of head CT scans, clinical data, laboratory results and culture results in children with suspected TBM spanning a period of four years (1998-2002) was performed at Red Cross War Memorial Children's Hospital. The selection criteria were designed to encompass all children with clinical features compatible with TBM who had undergone CT scans.

The final group of patients for the study was determined in the following manner: A laboratory database was searched for all patients who had CSF sent for TB culture. A CT scan database was searched to identify those patients who had CT scans of the head. The two database searches were then cross-matched. The patient's clinical notes were required to reflect clinical features compatible with any meningitis (criterion [Aiii] in Table 1) for inclusion. The clinical notes had to be complete and there also had to be a complete CSF chemistry analysis, as well as results of TB culture and CT scan of the brain, both without and with intravenous contrast. Patients were excluded when any of the CSF chemistry results, culture results or clinical notes was unavailable, incomplete or inadequate. Patients were also excluded when the CT scan of the brain was performed inappropriately (e.g. with incorrect windowing, without contrast medium or without a non-contrast study). The clinical and CSF criteria tabulated below (Table 1) are based on the existing protocol at the Red Cross Children's Hospital and were used by two paediatric neurologists blinded to the CT findings to group the patients into three categories of 'Definite', 'Probable' and 'Negative' TBM. These categories are defined below in the key to the table.

Key to the table below:

Definite TBM = [A (iii)] and culture positive CSF for TB [B (vi)]
(Clinical features of meningitis with gold standard diagnosis of TBM)

Probable TBM = [A (iii)] and 2 other positives from [A] and 3 positives from [B]
(Clinical features of meningitis and CSF chemistry for TB, but culture)

Negative = [A(iii)] but does not meet all the other criteria and an alternative diagnosis made by culture or trial of therapy.
(Clinical features of meningitis but CSF culture and chemistry negative).

Table 1: Inclusion criteria for the groups 'Definite TBM', 'probable TBM' and 'Negative' for this study (based on the clinical protocol of the Red Cross Children's Hospital Neurology Division)

A: Clinical:

i. Household TB contact
ii. Positive Mantoux over 15mm
iii. Neurological features: depressed level of consciousness, focal neurological signs, raised intracranial pressure, seizures or meningism
iv. Systemic upset (in combination with neurological findings), failure to thrive, fever, night sweats, proven pulmonary TB, proven abdominal TB, or evidence of extra-neurological involvement
v. Prolonged symptoms of over 48 hours

B: CSF

i. Pleocytosis (greater than 20 cells per mm^3) with lymphocyte predominance (>50%)
ii. Protein greater than age-specific normal value; especially > 1.0 mmol/l
iii. Chloride less than 120 mmol/l
iv. Glucose less than 60 % of blood level
v. Acid fast bacilli on stains; negative india ink stains for cryptococcosis
vi. Culture positive for TB

The table below is provided to give perspective on the restriction of patient numbers when strict inclusion criteria are used. The definite positive patient population is by definition CSF culture positive for TBM.

Table 2: Comparison of published series with regard to inclusion criteria

Study [reference]	Total no. patients with TBM in study who underwent CT	CSF culture +ve	CSF stain +ve	Other fluid culture +ve	Other fluid stain +ve	No. patients proven TBM	Total CSF culture and/or stain +ve
Artopoulos (1984)[37]	9					2	22%
Schoeman (1985)[52]	24	21%		17%		9	38%
Leiguarda (1988)[39]	65					20	30%
Schoeman (1988)[47]	27					6	22%
Gelabert (1988)[43]	26	81%				21	81%
Waeker (1990)[7]	30	37%	3%	10% (GA)	47%	12	40%
Altunbasak (1994)[41]	52	9.6%	7.6%	9.6% (GA)		14	26.9%
Schoeman (1995)[40]	198	15%		12% (GA)		54	27%
Kumar (1996)[46]	94					0	0%
Patwari (1996)[49]	136					0	0%
Schoeman (1997)[29]	141	16%		23%		56	39%
Kumar (1999)[9]	110	16%				18	16%
Farinha (2000)[10]	33	39%	51%			30	90%
Tung (2002)[8]	7					1	14%
Andronikou (2004)	37	100% (By definition)				37	100%

(GA) = gastric aspirate

All scans were performed on a General Electric (Yokohama Medical Systems, Japan) Prospeed Fast S Computed Tomography scanner. The scan technique was standardised, even though the study was retrospective, as all scans were performed according to a brain study protocol, including 5 mm slice thickness for the posterior fossa and 10 mm slice thickness above that level. Iodinated low osmolar intravenous iodinated contrast medium was administered at a prescribed dose of 1ml/kg body weight.

Three reviewers retrospectively assessed the CT scans, blinded to the final diagnosis, according to a predetermined set of criteria (given below), by consensus. One reviewer was a paediatric radiologist with a neuroradiology interest and extensive experience in TB imaging. The second reviewer was a junior consultant radiologist and the third a medical student trained for the research project. The two paediatric neurologists in the study carried out the case allocation independently.

The CT parameters specifically assessed included:

Primary Assessment Criteria

1] The presence or absence of hydrocephalus (subjectively evaluated)
2] The presence or absence of hyperdensity in the basal cisterns prior to contrast administration (subjectively evaluated)
3] The presence or absence of basal enhancement (subjectively evaluated)

Secondary Assessment Criteria

1] The presence of infarcts
2] The site of infarcts
3] The site of basal enhancement
4] The site of non-contrast hyperdensity
5] Hydrocephalus distinguishable from atrophy
6] Changes on follow-up CT within one month of initial CT (when performed)

Non-contrast density:

As non-contrast cisternal hyperdensity is a new sign of TBM, it was felt important to validate its detection.

Visual impression:

The CT scans were assessed retrospectively on film ('hard copy'). Computer data were not available for direct measurement on the CT scanner. The presence of hyperdensity was assessed subjectively by the reviewers by comparing this density to adjacent brain structures including the basal ganglia, cortex, white matter and CSF which normally fills cisterns and is of low (water) density on CT. Hyperdensity was recorded when the density of the cisternal contents, including any of the suprasellar cistern, the middle cerebral artery cisterns, the interpeduncular cistern, the ambient cisterns and / or the Sylvian cisterns, was equal to or above that of normal cortex (grey matter), either in part or in entirety as a whole.

Computerised assessment:

An objective method was used to validate the visual impressions. A student in the Division of Biomedical Engineering of the University of Cape Town designed a software package for a Master's thesis. The hard copies of patients thought to demonstrate hyperdensity on non-contrast studies (numbered patients 1 to 17) were digitised using a professional X-ray film scanner. The software package allowed conversion of the optical density recorded on the films back to Hounsfield units. This was achieved by calibration of the grey scales printed on individual films against the recorded window levels to generate lookup tables. The calculation of the density of regions of interest was performed by interpolation against the lookup table.

At least seven measurements (the maximum allowed by the computer software) were taken in the suspected hyperdense areas at each individual scan level. The 2 highest readings were recorded. Multiple density readings were also taken from normal areas of the cortex (carefully avoiding any areas of peripheral beam-hardening and posterior fossa

structures), the basal ganglia (as these are also grey matter structures, much like cortex) and the CSF. The highest readings were again recorded.

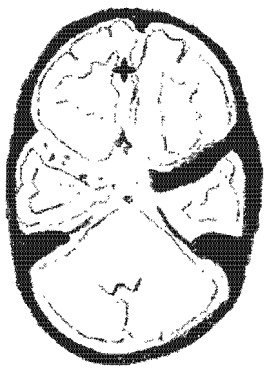

Fig 1:The '+'represents the usual location where a normal cortical density reading was taken. (The frontal cortex near the falx is away from the effects of beam-hardening arising at the calvarium, which can artefactually increase the density reading).

The densities of the normal areas and the abnormal basal cisterns were compared. A 'low threshold' level was set at the lower of the density readings recorded in the abnormal areas and a 'high threshold' level was arbitrarily set 4 Hounsfield units above this value. An image was then created using the densities between the two threshold levels as the window width. Applying the software threshold function, which removes any densities not within the high and low threshold values, did this. The resultant images were reviewed to confirm the visual impressions on the original scans (refer to the Results section below for the images created by this method).

Statistical analysis:

Sensitivity, specificity, positive predictive value, negative predictive value and likelihood ratios were calculated for individual radiological features, as well as for combinations of radiological features, compared with the diagnosis of definite TBM. Categorical data were reported as proportions. Hypothesis testing was performed using the Fisher Exact Test and Chi Squared Test where appropriate.

Results:

The initially selected group comprised 353 patients who had both CSF sent for TB culture and had undergone CT spanning a period of 4 years. One hundred and ninety one patients were excluded (38 because of absent clinical notes, 95 because of incomplete CSF data, 29 because of incomplete clinical data, 28 because of incomplete or inadequate CT scans [10 of which were definite TBM] and 1 patient with atypical mycobacterium meningitis). The remaining 162 patients fell into three groups according to CSF culture and chemistry results, as defined above.

The 'Definite' TBM group comprised 37 children:

16 females and 21 males, with a mean age of 24 months (4.3-144 months).

Twenty-six of the definite TBM patients presented in Stage II (MRC United Kingdom) and the remainder presented in Stage I and III.

The 'Negative' group of 32 children was made up of 17 females and 15 males, and had a mean age of 18 months (10-120 months). The alternative diagnoses included 20 patients with bacterial meningitis, 8 with viral meningitis, 1 patient with aseptic meningitis, 1 patient with cryptococcosis, 1 with HIV encephalopathy and 1 patient with a stroke who did not have meningitis.

The '**Probable group**' consisted of 93 patients

Detailed statistical analysis for the 'Definite' TBM and 'Negative' groups is presented in Table 3 below, indicating sensitivity, specificity, positive predictive value, negative predictive value and likelihood ratio for each CT feature of TBM. Simple numeric results for the 'Probable' group are presented for completeness in Table 4 below.

Table 3: The CT results of patients in each group are tabulated below:

CT feature	Definite TBM (37)	Negative TBM (32)	Sensitivity (%)	Specificity (%)	Positive predictive value	Negative predictive Value	Likelihood ratio +ve	Likelihood ratio -ve
Hydro-cephalus	25 (67.6%)	9 (28.1%)	68	72	74	66	2.4	0.45
Infarcts	23 (62.2%)	7 (21.9%)	62	78	77	64	2.8	0.48
Non-contrast density	17 (46%)	0	46	**100**	**100**	62	N/A	0.54
Basal Enhancement	33 (89.2%)	2 (6.3%)	89	94	94	88	14.3	0.12
Granuloma	5 (13.5%)	2 (6.3%)	14	94	71	48	2.2	0.92
'Classic triad'	15 (40.5%)	0	41	**100**	**100**	59	N/A	0.59

Key: 'Classic triad' = basal enhancement plus infarction plus hydrocephalus

N/A = Not Applicable as these values are not statistically calculable

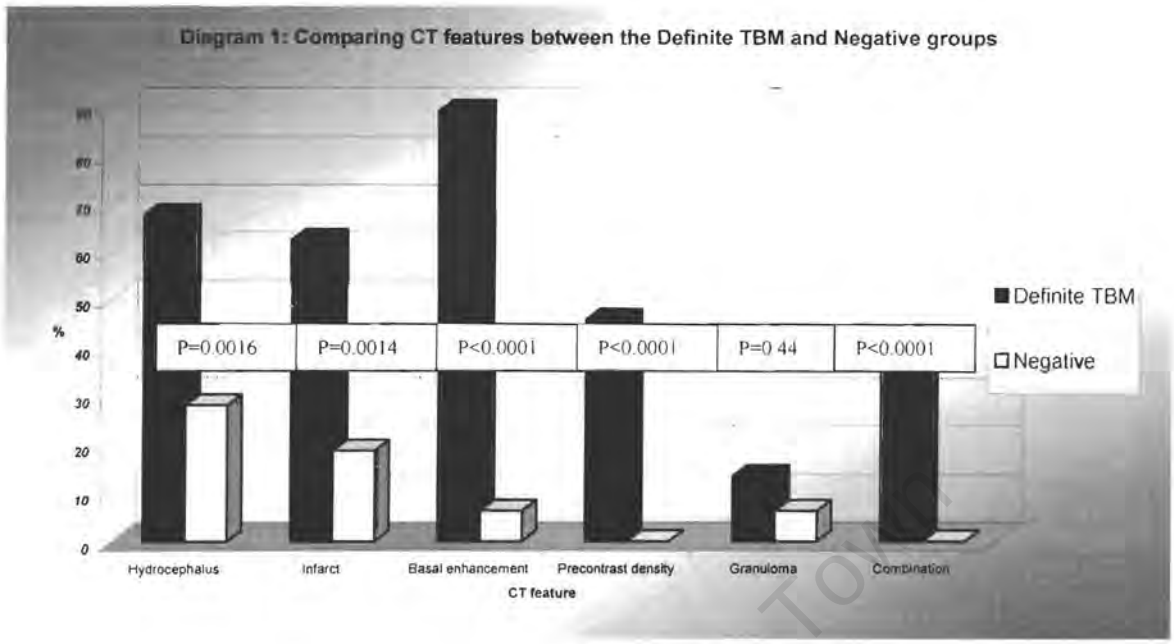

Table 4: Results of the '**Probable**' group (93 children).

CT feature	Probable (93)
Hydrocephalus	56 (60.2%)
Infarcts	50 (53.8%)
Basal enhancement	62 (66.7%)
Non-contrast density	43 (46.2%)
Granuloma	25 (26.9%)
Combination	32 (34.4%)

The 'Probable' group was only used for further comparison with regard to non-contrast density distribution where it was felt to add value. Only the definitely positive and definitely negative patients for TBM were used for the main statistical analysis, so that the groups would remain 'pure'.

Results of computerised measurement of hyperdensity in the cisterns on non-contrast CT:
The non-contrast density was subjectively determined to be present in 17 patients. Figures 2 – 18 demonstrate the non-contrast CT scans of these patients, with accompanying images of a high and low-density thresholds applied, as described in the 'Methods' section. This technique results in only the cisternal hyperdensity and 'beam-hardened' cortex being demonstrated. Density was confirmed using the computerised quantitative method described above in all 17 patients. The derived Hounsfield units of the hyperdense areas are compared to normal parenchyma, basal ganglia and CSF in tables 5 and 6. (Computerized measurement was not undertaken in patients in whom cisternal hyperdensity was not subjectively identified). Table 7 compares distribution of non-contrast high density in the 'Definite' and 'Probable' groups.

Table 5: Density readings of normal and abnormal areas in the seventeen patients considered to show cisternal hyperdensity on non-contrast CT

Patient Number	Maximum non-contrast density 1	Maximum non-contrast density 2	Average cisternal non-contrast density	Basal ganglia	Parenchyma	CSF
1	46.5	46.3	46.4	40.9	42.6	15.6
2	43.5	45	44.3	36.6	40.8	12.1
3	39.5	40.9	40.2	31.9	28.2	10.8
4	42.5	41	41.8	33.9	37.8	12.7
5	39	39.5	39.3	36.2	37	7.9
6	39.4	39	39.2	29.5	34.6	7.7
7	40.7	42.3	41.5	35.5	37.2	11
8	37.5	36.7	37.1	29.5	31	3.5
9	43.9	41.4	42.7	37.7	38.6	13.4
10	35.5	37.7	36.6	31	32.7	7.3
11	52.4	45.5	49	38.7	41.1	16.9
12	41.2	40.5	40.9	30.9	39.5	13.2
13	42.3	42.1	42.2	35.6	39.4	12.7
14	38.4	37.3	37.9	32.1	33.9	7.7
15	44.3	43.3	43.8	35.5	39.7	9.9
16	38.2	36.1	37.2	30.6	35.3	7.4
17	39.4	38.2	38.8	29.6	33.8	7.5
Average	**41.4**	**40.8**	**41.1**	**33.9**	**36.7**	**10.4**

Table 6: Differences between the highest abnormal density and the highest and lowest normal density:

Patient Number	Minimum difference between highest abnormal and highest normal parenchymal or basal ganglia density	Maximum difference between highest abnormal and lowest normal density parenchymal or basal ganglia density
1	3.9	5.6
2	4.2	8.4
3	9	12.7
4	4.7	8.6
5	2.5	3.3
6	4.8	9.9
7	5.1	6.8
8	6.5	8
9	5.3	5.3
10	5	6.7
11	11.3	13.7
12	1.7	10.3
13	2.9	6.7
14	4.5	6.3
15	4.6	8.8
16	2.9	7.6
17	5.6	9.8
Average	**5**	**10**

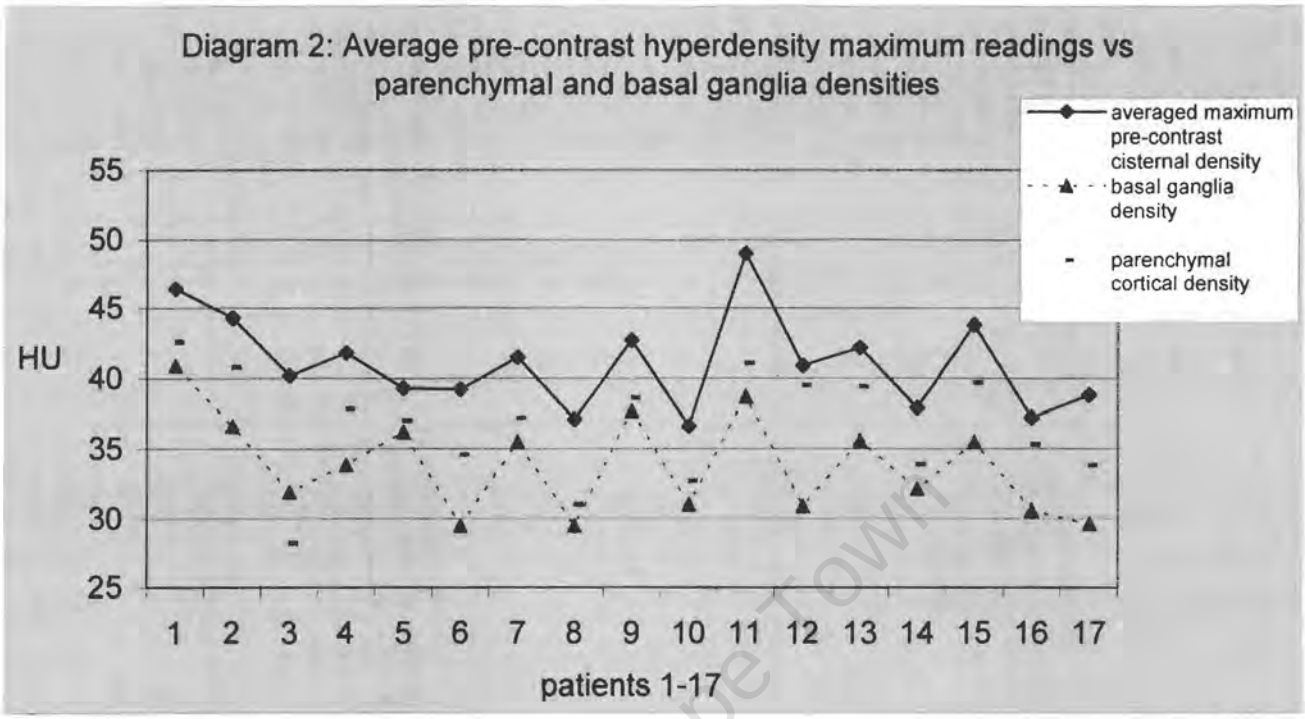

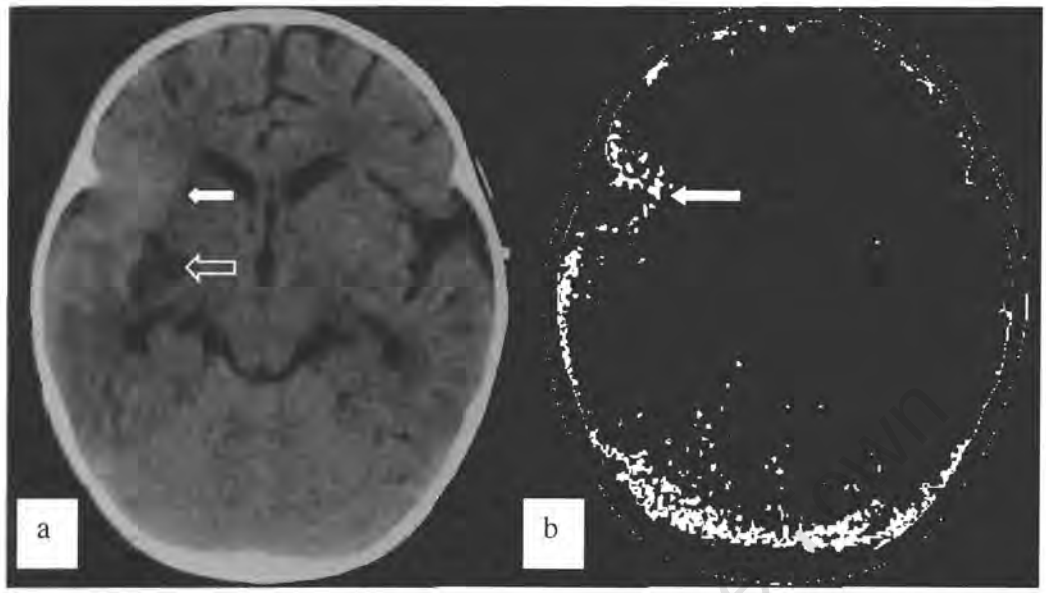

Figure 2 a and b: Patient 1 demonstrates hyperdensity in the right Sylvian fissure (white arrow) on non-contrast CT (a), and confirmed on the image with high and low density threshold (b). There is also infarction in the subcortical white matter deep to the insula on the right (open arrow).

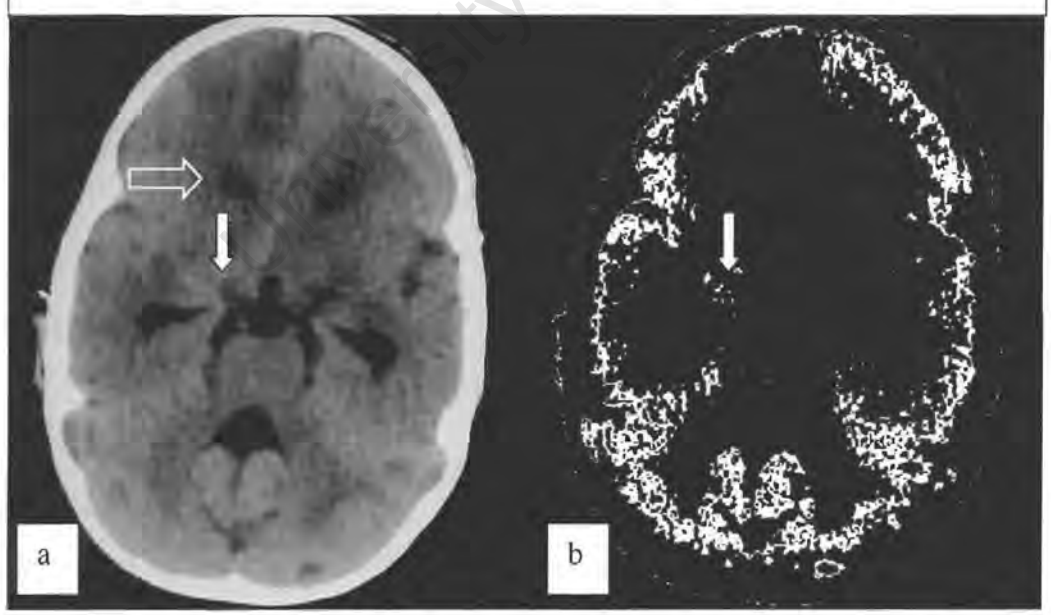

Figure 3 a and b: Patient 2 demonstrates hyperdensity in the right middle cerebral artery cistern (white arrow) on non-contrast CT (a) and confirmed on the threshold image (b). Cortical infarction is present in the right frontal lobe (open arrow), and there is also moderate hydrocephalus.

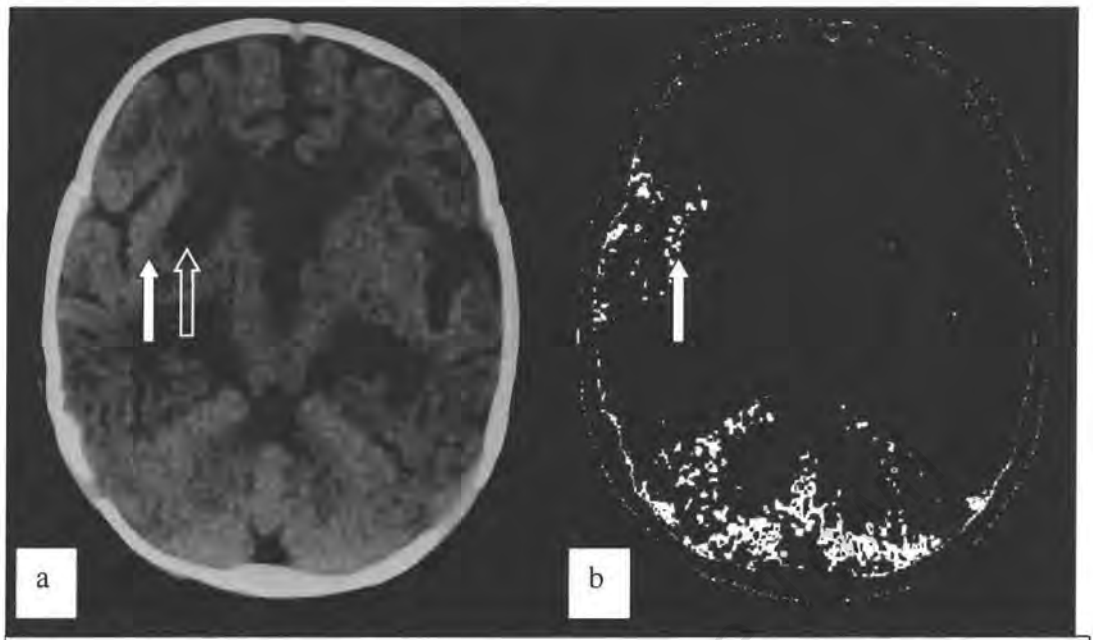

Figure 4 a and b: Patient 3 demonstrates hyperdensity in the right Sylvian cistern (white arrow) on non-contrast CT (a) and confirmed on the threshold image (b). There is also an infarction involving the right lentiform nucleus (open arrow).

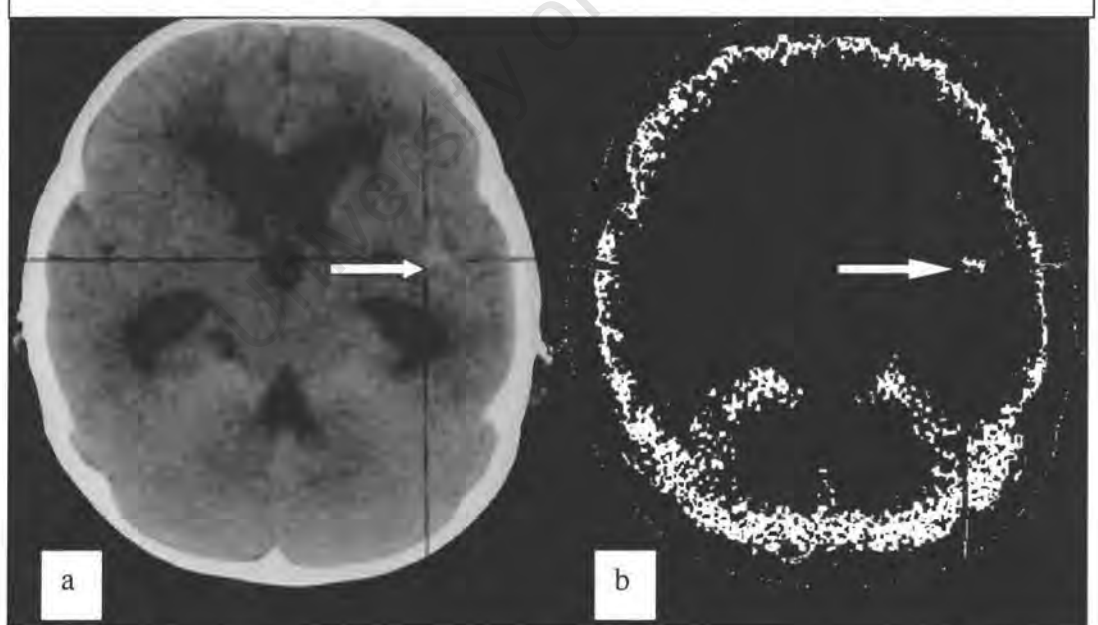

Figure 5 a and b: Patient 4 demonstrates hyperdensity in the left Sylvian cistern (arrow) on non-contrast CT (a), confirmed on the density threshold image (b). The caudate and lentiform nuclei bilaterally are of lower density than the cortex in keeping with infarction. Hydrocephalus is also present.

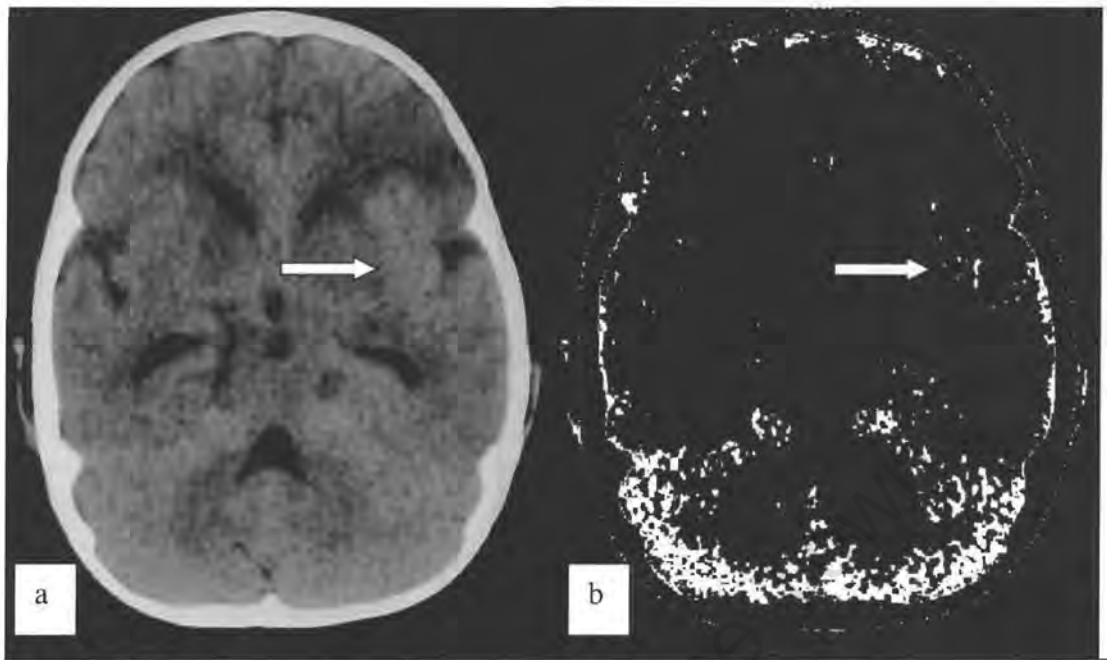

Figure 6 a and b: Patient 5 demonstrates hyperdensity in the left Sylvian cistern (arrows) on non-contrast CT (a), confirmed on the density threshold image (b).

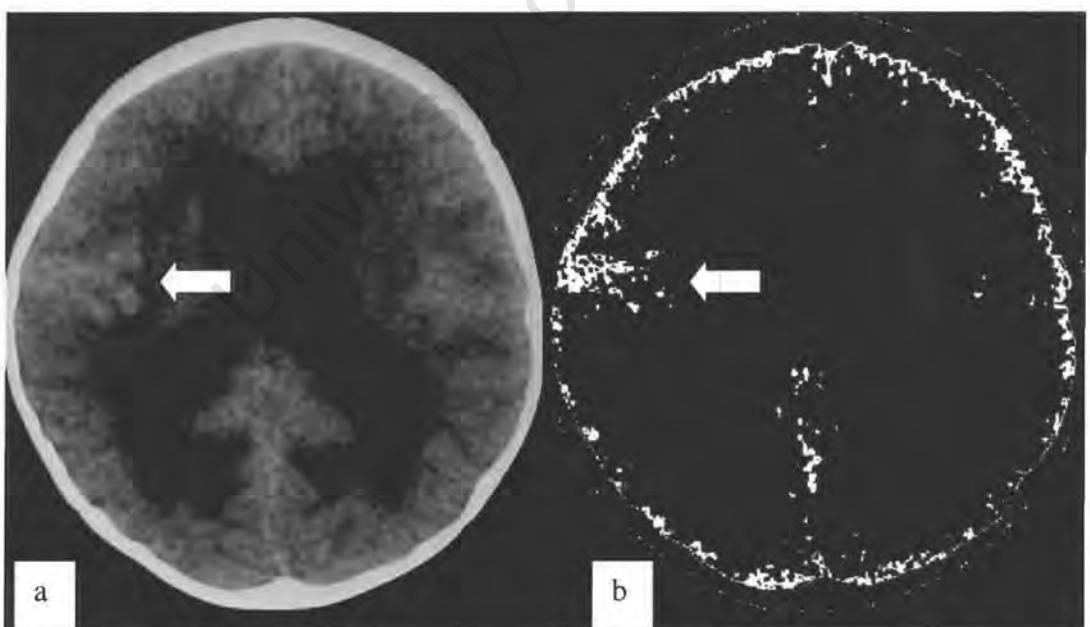

Figure 7 a and b: Patient 6 demonstrates hyperdensity in the right Sylvian cistern (arrows) on non-contrast CT (a), confirmed on the density threshold image (b). There is accompanying hydrocephalus.

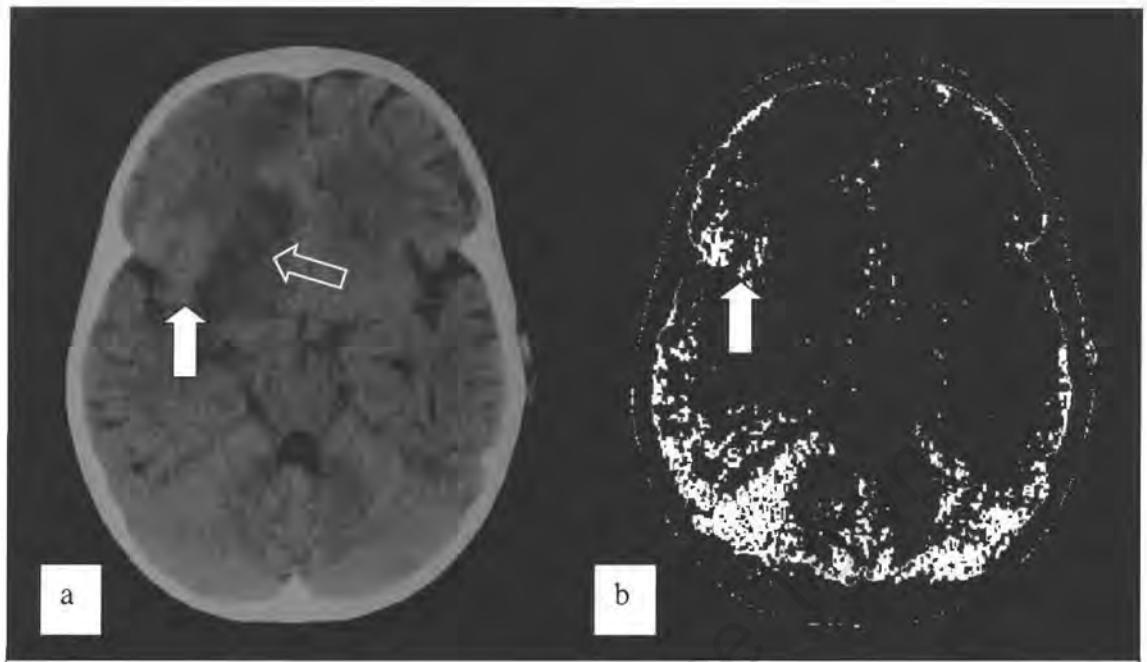

Figure 8 a and b: Patient 7 demonstrates hyperdensity in the right Sylvian cistern (white arrows) on non-contrast CT (a), confirmed on the density threshold image (b). Note adjacent right frontal low density infarction (open arrow).

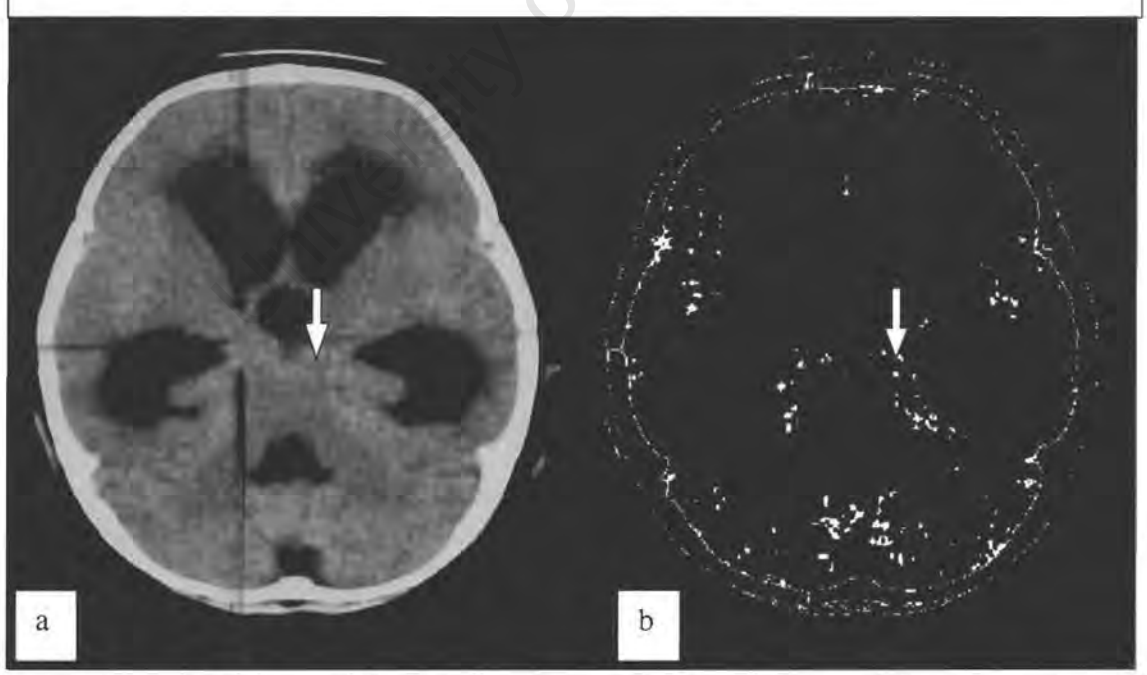

Figure 9 a and b: Patient 8 demonstrates hyperdensity in the posterior portions of the suprasellar cistern, ambient cisterns (arrows) and Sylvian cisterns on non-contrast CT (a), confirmed on the density threshold image (b). There is also severe

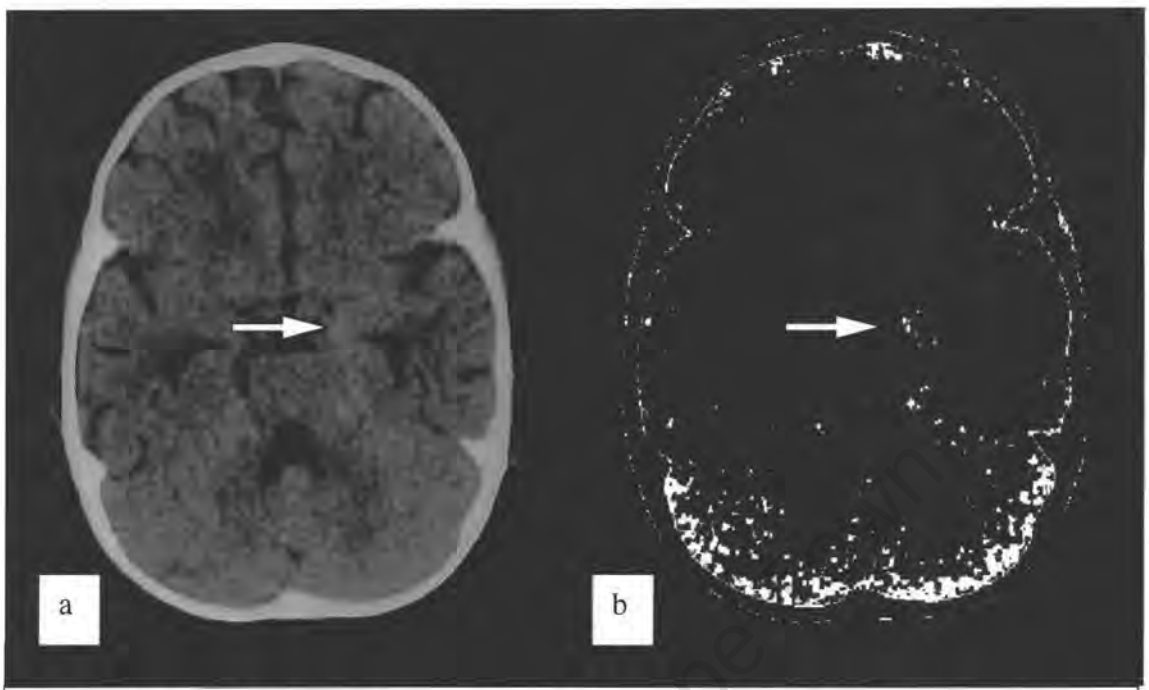

Figure 10 a and b: Patient 9 demonstrates hyperdensity in the left side of the supra sellar cistern (white arrows) on non-contrast CT (a), confirmed on the density threshold image (b).

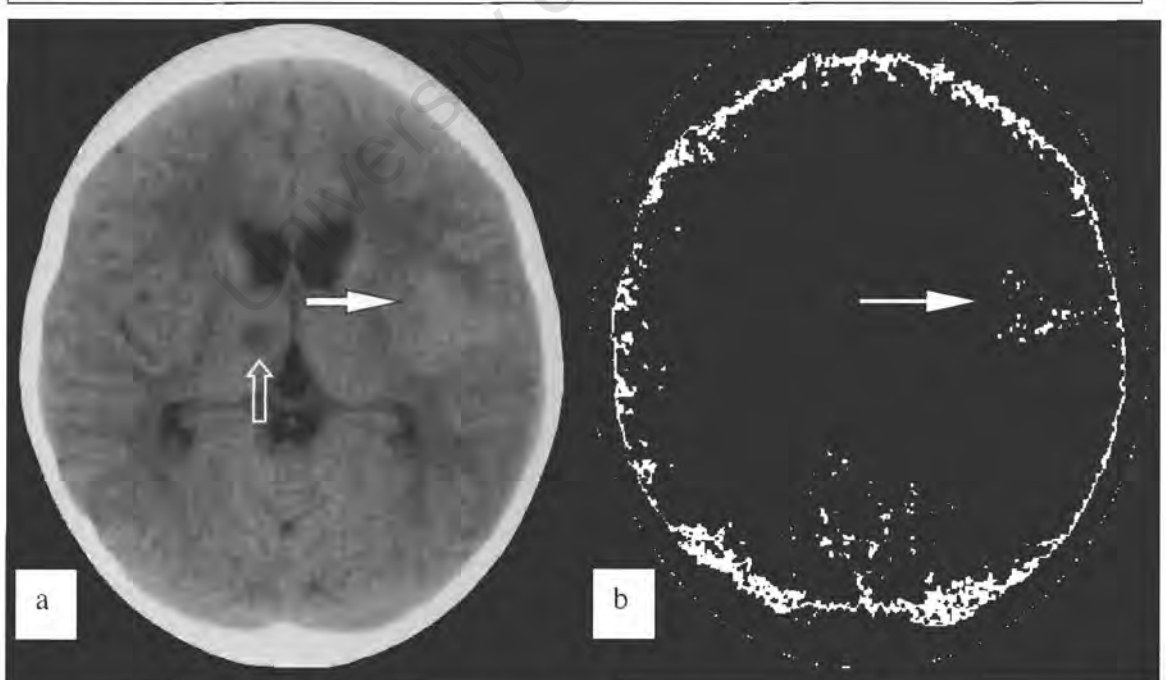

Figure 11 a and b: Patient 10 demonstrates hyperdensity in the left Sylvian cistern (white arrows) on non-contrast CT (a), confirmed on the density threshold image (b). There is focal infarction involving the contralateral thalamus (open arrow).

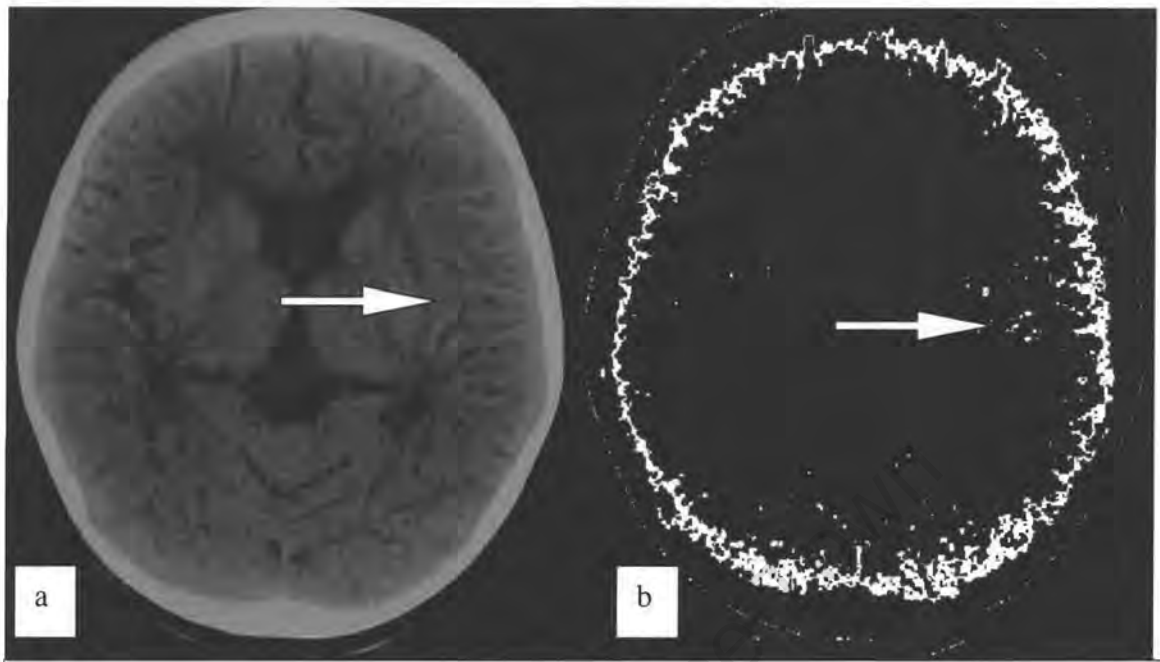

Figure 12 a and b: Patient 11 demonstrates hyperdensity in the left Sylvian cistern (white arrows) on non-contrast CT (a), confirmed on the density threshold image (b).

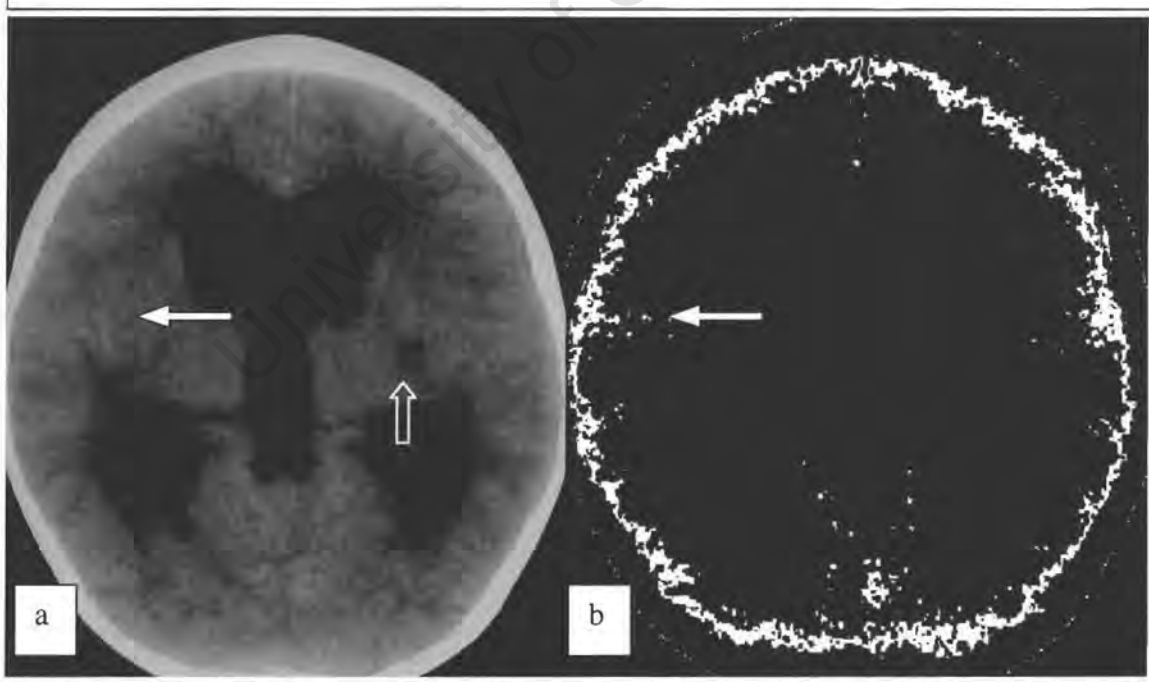

Figure 13 a and b: Patient 12 demonstrates hyperdensity in the right Sylvian cistern (white arrows) on non-contrast CT (a), confirmed on the density threshold image (b). There is accompanying severe hydrocephalus and a contralateral internal capsule infarction (open arrow).

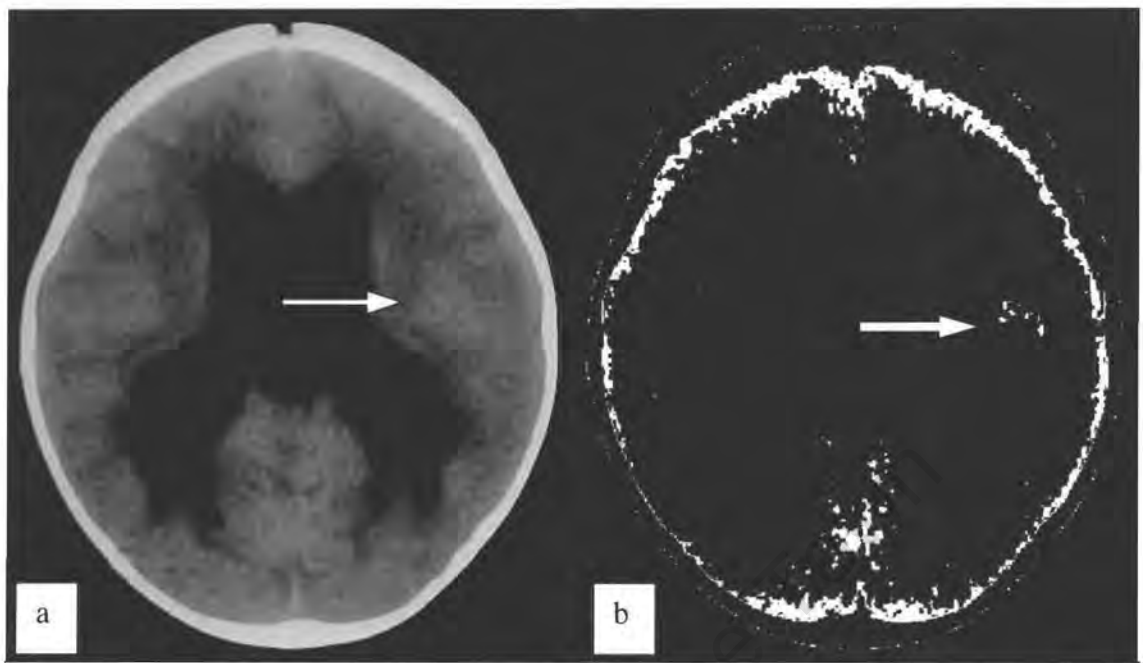

Figure 14 a and b: Patient 13 demonstrates hyperdensity in the left Sylvian cistern (white arrows) on non-contrast CT (a), confirmed on the density threshold image (b).There is also severe hydrocephalus.

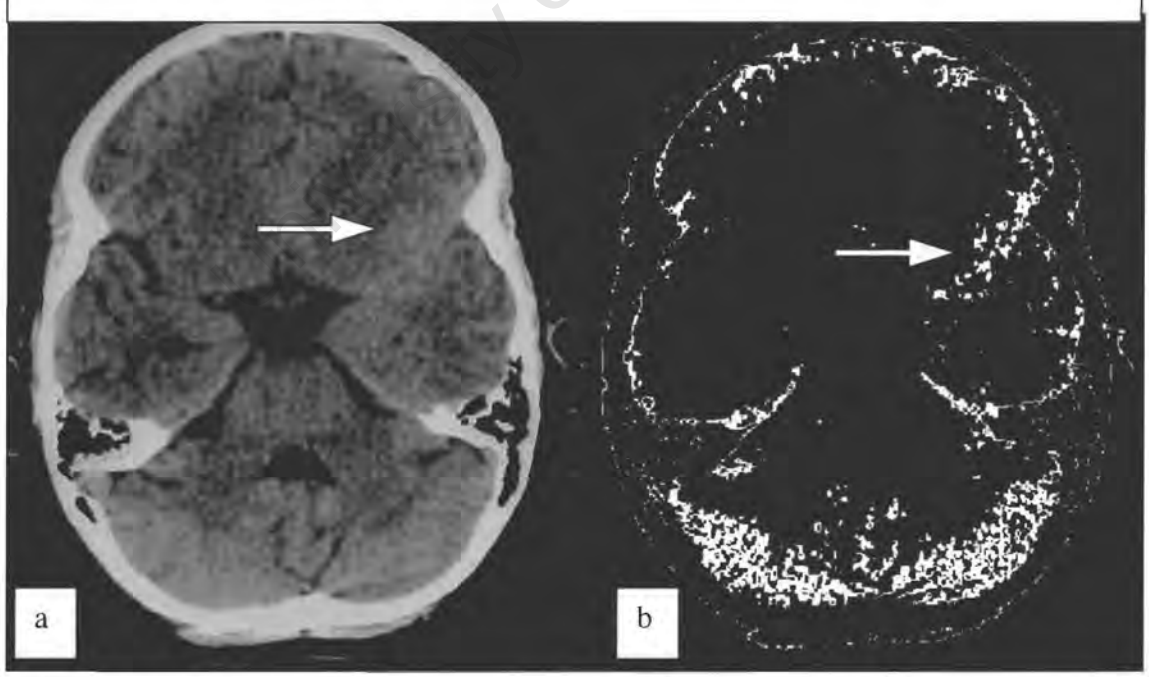

Figure 15 a and b: Patient 14 demonstrates hyperdensity in the left middle cerebral artery cistern (white arrows) on non-contrast CT (a), confirmed on the density

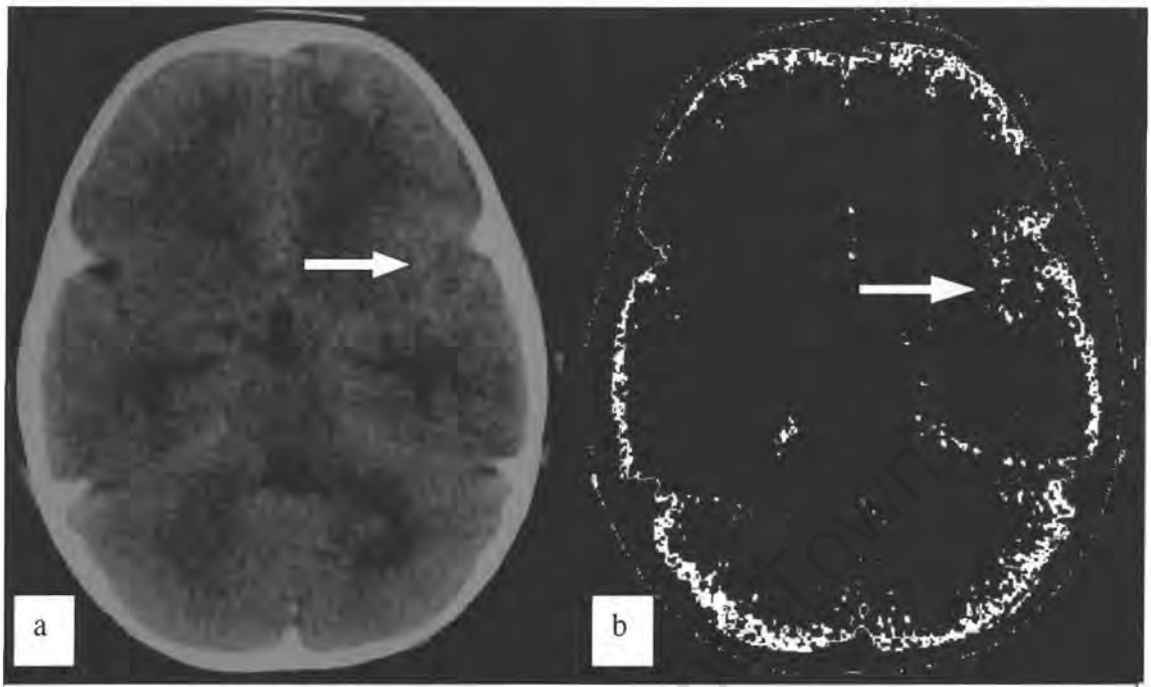

Figure 16 a and b: Patient 15 demonstrates hyperdensity in the left Sylvian cistern (white arrows) on non-contrast CT (a), confirmed on the density threshold image (b)

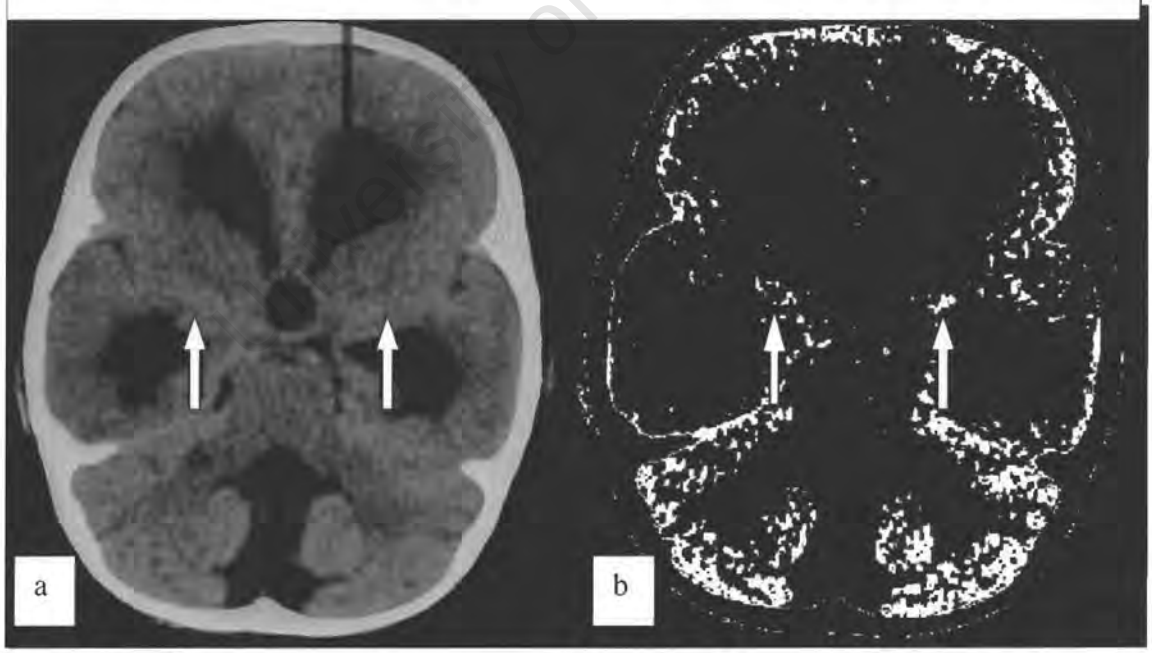

Figure 17 a and b: Patient 16 demonstrates hyperdensity in both middle cerebral artery cisterns (arrows) on non-contrast CT (a), confirmed on the density threshold image (b). There is also significant accompanying hydrocephalus.

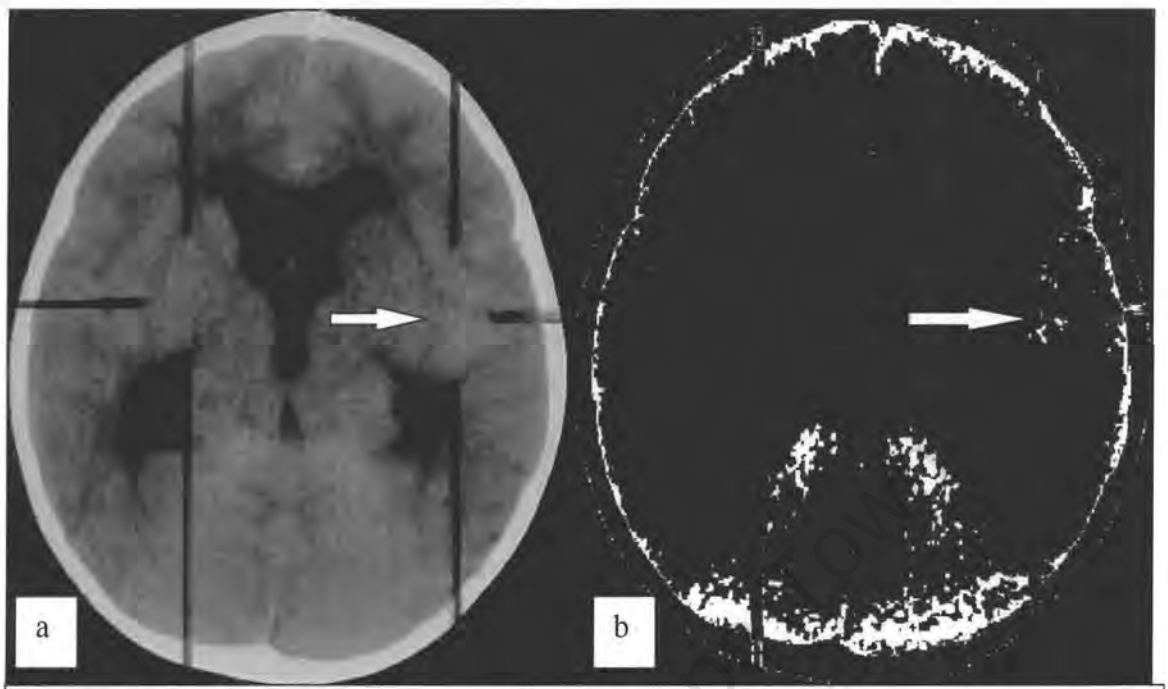

Figure 18 a and b: Patient 17 demonstrates hyperdensity in the left Sylvian cistern (arrows) on non-contrast CT (a), confirmed on the density threshold image (b). There is accompanying hydrocephalus.

Table 7: Distribution of the cisternal high density in 'Definite TBM' group compared to the patients in the 'Probable' group on non-contrast CT.

Distribution of non-contrast hyperdensity	**Definite TBM (17)**	**Probable TBM (41)** (films of 2/43 patients not available during review period)
Right only (uni- or multifocal)	2 (12%)	9 (22%)
Left only (uni- or multifocal)	4 (24%)	10 (24%)
Unifocal	6 (35%)	15 (37%)
Right	2 (12%)	7 (17%)
Left	4 (24%)	6 (15%)
Midline	0	2 (5%)
Multifocal	**11 (65%)**	**26 (63%)**
Symmetrical	6 (35%)	11 (27%)
Asymmetrical	5 (29%)	15 (37%)
Right only	0	2 (5%)
Left only	0	4 (10%)
Bilateral	9 (53%)	16 (39%)
Midline only	0	2 (5%)
Unilateral and midline	2 (12%)	2 (5%)
Diffuse (suprasellar cistern and extensions plus Sylvian and ambient)	3 (18%)	0
Specific locations involved		
Anterior cerebral artery cistern	8 (47%)	14 (34%)
Right middle cerebral artery cistern	9 (53%)	15 (37%)
Left middle cerebral artery cistern	9 (53%)	16 (39%)
Right ambient cistern	5 (29%)	9 (22%)
Left ambient cistern	6 (35%)	10 (24%)
Central suprasellar cistern	8 (47%)	13 (32%)
Interpeduncular cistern	5 (29%)	6 (15%)
Right Sylvian cistern	9 (53%)	19 (46%)
Left Sylvian cistern	10 (59%)	24 (59%)

The distribution of non-contrast density in the cisterns was predominantly multifocal for both Definite and probable groups (65% and 63% respectively). The most frequent locations for both groups were the Sylvian cisterns (predominantly the left), followed by the middle cerebral artery cisterns, anterior cerebral artery cisterns and the suprasellar cistern centrally.

Discussion:

CT Features of TBM

The CT features of TBM, specifically hyperdensity on non-contrast studies, basal enhancement and hydrocephalus are discussed below in detail. Comparisons of our results of these and the other CT features of TBM are provided in the tables below. Table 8 compares our results to other paediatric series, while Table 9 compares our results to previous adult series.

CT Features of TBM – exudates on non-contrast studies

A few authors have inferred the presence of basal exudates prior to contrast administration (figure 19a and b) by recognising obliteration of the basal cisterns [15-17,27,33], presumably by isodense material obscuring the outline of the adjacent brain cortex [16,27,33]. These areas may or may not enhance after intravenous administration of iodinated contrast medium (figure 20 a and b) [15,17,27,33]. Only two authors have referred to hyperattenuating / hyperdense exudates within the basal cisterns and Sylvian fissures on CT scanning of patients with TBM [3,26]. Rovira et al have this finding as representing fibrogelatinous exudates in the early phase of TBM and state that this is common in infants with TBM [26]. De Castro et al comment that CT scanning usually demonstrates isoattenuating or hyperattenuating basal cisterns on non-contrast scans. Neither of these authors reported the incidence of this finding, further explored the reason for the CT density, or correlated it with other findings.

There are a number of reports stating that the presence of an exudate seen on CT (as determined by the presence of basal enhancement) is associated with a poor prognosis [8,33,36]. Likewise the amount and density of the exudates are also proposed to reflect a poor outcome [33,36]. Others indicate that non-enhancing (isodense) exudates have a good outlook, while enhancing exudates have a bad prognosis [27]. A literature search of English language journals on Medline using the search phrases 'TBM', 'tuberculous meningitis', 'computerised tomography', 'computerized tomography', 'CT', 'hyperdensity', 'cistern' and 'basal cistern' revealed one 'Case of the day' report of an

infective agent other than TB causing density within the cisterns on non-contrast CT. In this case the author proposed a haemorrhagic exudate as the cause for this appearance in a single case of Neisseria meningitis [73]. A limited number of other conditions produce high density in the subarachnoid cisterns on non-contrast CT. These are acute subarachnoid haemorrhage (acute) and a water-soluble contrast from myelography performed 1-2 days before the CT [73]. Bayes theorem should be kept in mind however, as the incidence of other possible causative agents of hyperdense exudates is low in our community (e.g. other granulomatous meningitides).

Precontrast cisternal hyperdensity is more specific in our study than any other single reported CT feature of TBM, with a specificity of 100% and a positive predictive value of 100, ruling the disease in. The sensitivity is low however. The difference in the presence of non-contrast cisternal density between the 2 groups of patients was statistically significant ($p<0.0001$). The highest abnormal hyperdensity reading was 46.5 HU, while the highest normal brain density reading was 42.6 HU. The lowest abnormal hyperdensity value recorded was 35.5 HU and the lowest normal cortical or basal ganglia density recorded was 32.7 HU. However, **in the same patient,** the non-contrast abnormal hyperdensity HU readings were always higher than the highest normal cortical or basal ganglia recordings by an average of 4.4 and 7.2 HU respectively, with a range of 5 to 10 HU (using the highest abnormal density readings).

The images created by density-thresholding (described in the methods section above) for the patients with subjectively determined non-contrast hyperdensity are presented in the 'Results' section above (arrows indicate areas of hyperdensity). Note that the peripheral cortical and posterior fossa structures (which are subject to beam hardening artefact) also form part of the image. The abnormal hyperdensity is typically visible centrally and often asymmetrically within the basal cisterns and Sylvian fissures, which should normally be of CSF density, and should therefore not contribute to the modified image. More often the hyperdensity is multifocal, and may be symmetrical or asymmetrical. The feature is most often identified at the Sylvian cisterns and middle cerebral artery cisterns, but is also seen regularly in the suprasellar cistern centrally, or in the anterior cerebral artery cistern. It is only rarely seen as a diffuse density involving all the cisternal spaces.

Automated or semi-automated methods of detection of the hyperdensity such as the technique described above should allow rapid and accurate diagnosis on the non-contrast study. This would save in resources and time by avoiding the need for a post-contrast study.

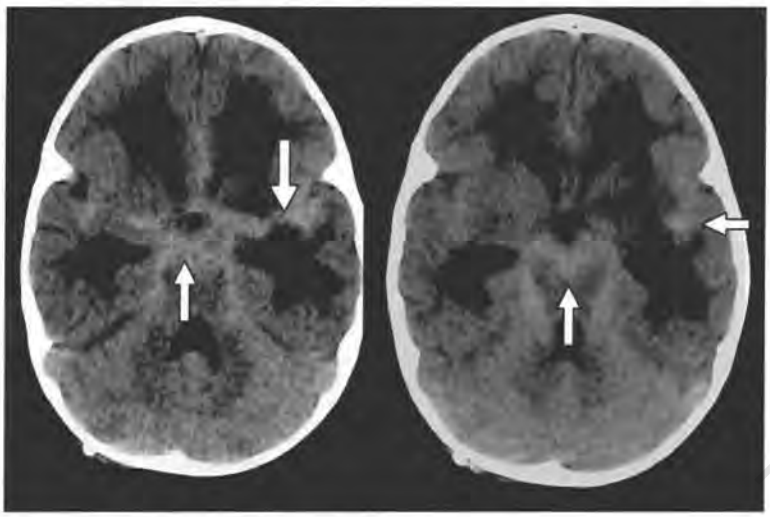

The hyperdense exudate or granulation tissue fills the suprasellar cistern and extends into the Sylvian and ambient cisterns in a patient from the 'Probable group'

Fig 19 a & b: Non-contrast hyperdensity in the cisterns

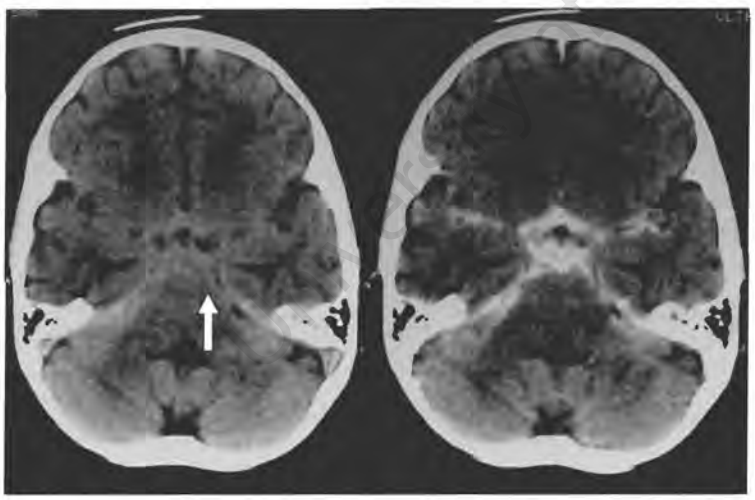

The non-contrast study demonstrates hyperdense material filling the suprasellar cistern (arrow) in a patient from the '**Probable**' TBM group. This material enhances prominently with contrast and probably represents richly vascularised granulation tissue. Another theory is that there is leakage of contrast medium from the intravascular compartment to lie within the exudates in the extravascular compartment.

Fig 20 a & b: Non-contrast cisternal hyperdensity enhancing after intravenous contrast

CT Findings – Basal Enhancement

Although lacking satisfactory pathophysiological confirmation, tuberculous meningitis is generally accepted to be the cause of the marked basal cistern contrast enhancement on CT in TBM [47]. The presence of the exudates (described in the Pathology section) is usually inferred on CT by the presence of contrast enhancement within the basal cisterns with an image resembling that obtained by the injection of contrast into the subarachnoid space (figures 21 – 28) [18,26,27,34]. Meningeal enhancement is also considered a sensitive CT pointer of TBM [7,17]. Enhanced demarcation of the basal meninges is said to be visible when there is granulation tissue in the basal cisterns [22,28]. Jinkins et al showed that during dynamic contrast enhanced CT in TBM, a rapid enhancement pattern is present a few seconds after the bolus injection, followed by an elevated plateau phase. They explained this as reflecting hypervascularity, with the later changes indicative of extra-vascular leakage of contrast [74]. It is therefore believed that basal enhancement may be due three factors occurring independently or in combination:

- Meningeal hypervascularity
- Leakage of contrast medium into the cisternal exudates
- Enhancement of the granulation tissue in the later stages
- [The non-contrast density may contribute to the post contrast density]

According to some authors, basal enhancement of the cisterns has not been documented in pyogenic (bacterial) meningitis [9,34], but there are others who consider the finding as being 'non-specific' and present in approximately 50% of bacterial meningitides [60], as well as in other granulomatous meningitides such as torulosis [34] and sarcoid. (Bayes Theorem is relevant to our research as the incidence of TBM in our population is high, while the incidence of fungal meningitis and sarcoidosis is low).

Most authors report basal enhancement as second in frequency on CT after hydrocephalus [8,15,27], with an incidence ranging from 75% to 92% [9,15,18,27,32,33]. Only one author reports that it is the most common finding (64%) on CT in TBM [28]. There are no defined objective criteria for determining the presence of basal enhancement

on CT, and even though some authors attempt to grade severity, this is based on subjective parameters [33,40,71].

The grading system used by Schoeman et al. [40] for basal enhancement is as follows:
-Grade 1 = **slight**: just visible
-Grade 2 = **moderate**: visible, but not filling the subarachnoid space
-Grade 3 = **severe**: cisterns appear obliterated

The grading system used by Bhargava et al [33] is as follows:
-**Mild**: cistern obliteration but no enhancement
-**Moderate**: high attenuation outlining and obliterating cisterns (post-contrast)
-**Severe**: copious, dense exudates with high attenuation, filling and expanding the cisterns

It is often difficult to differentiate normal enhancement of the vessels of the circle of Willis (figure 29 and 30) from abnormal cisternal enhancement, especially in the presence of severe hydrocephalus. Hydrocephalus compresses the basal cisterns causing the cerebral lobes to lie close to one another, frequently complicating separation of normal vessels from possible abnormal meningeal enhancement. It has been suggested that the low incidence of basal enhancement in one series of TBM patients was possibly due to the low dose of contrast medium employed. The study used 1ml/kg, which is the standard dose in our institution. However the scans were also performed in 1978 when CT was in its infancy and the resolution and sensitivity of the CT scanner may have been the major limiting factor [19]. Teo et al also suggest that the detection of basal enhancement may be affected by the (relative) volume of contrast medium administered [28]. Abnormal basal enhancement has been noted to be irregular in outline and quite different from the sharply defined enhancement of the vessels of the circle of Willis [28]. Moreover, some reports indicate that basal enhancement increases during the course of the illness, and is often seen after initiation of anti-TB treatment [18] as well as on follow-up without any apparent change in the patient's condition [18,28]. The commonest sites of basal enhancement are the suprasellar, ambient and Sylvian cisterns [16,18,30,32,33,71], ranging from 60% to 80% [33]. Co-existing HIV infection also

affects the presence of basal enhancement according to one study, with basal enhancement significantly more common and more prominent in HIV-negative than in HIV-positive patients [5].

We found that basal enhancement was the most common finding, seen in 89% of definite TBM patients in our series. It was more common than hydrocephalus, which was present in 67.6%, while infarcts were seen in 62.2% of patients. Basal enhancement had a sensitivity of 89% and a specificity of 94%, with a positive predictive value of 94 and a likelihood ratio of 14.3. This means that a patient not showing basal enhancement is unlikely to have TBM i.e. it is useful for ruling out the disease. Basal enhancement is also convincing evidence that the disease is TBM, based on the likelihood ratio. There was also a statistically significant difference for the presence of basal enhancement between the definite and negative groups of patients ($p<0.0001$). Moreover, some features of bacterial meningitis such as CSF-density non-enhancing surface collections, were not seen in any patients with TBM (figure 31).

All our patients with non-contrast density in the basal cisterns showed basal enhancement after contrast administration. The presence of basal enhancement and non-contrast density were correlated with other CT detectable complications of TBM, namely hydrocephalus and infarction within the 'Definite' group. Ninety-six percent of patients with hydrocephalus and 96% of patients with infarction had abnormal basal enhancement in our study.

Contrast enhanced MRI is known to be more sensitive than CT for identifying basal enhancement. MRI readily differentiates the basal cistern enhancement from the flow voids within normal vessels of the circle of Willis in patients with equivocal CT enhancement (figure 32 a and b) [30]. On T-2 weighted images, loss of normal CSF signal in the subarachnoid cisterns is assumed to represent exudates and fibrosis ("arachnoiditis"), but was seen in only 18.5% patients in one study [40]. There are no specific MRI attributes of the exudates that have been reported for TBM [40]. As mentioned previously, it is not feasible to perform MRI on all patients with suspected

TBM in our setting. This is because patients usually present in Stage II and need rapid imaging, which is often not possible on MRI, given the poor availability of MRI (the unit is 'off-site' at our facility) and MRI compatible life-support systems.

A similar threshold programme to the one used for detecting hyperdensity in the cisterns may be useful for detecting basal enhancement. This is also being devised as part of a related research project. Subtraction techniques using the non-contrast study as a mask, with resultant images representing only the enhancing areas are also being investigated (figure 33 a and b).

HIV positive patients may not demonstrate the same frequency or degree of enhancement due to an inability to mount an immune response and generate the granulomatous exudates [5,13]. Our patient group was collected retrospectively and very few patients had undergone HIV testing, relating to strict legislation requiring informed consent for this. We cannot determine to what extent HIV may influence the profile of our findings.

Patterns of Basal Meningeal Enhancement

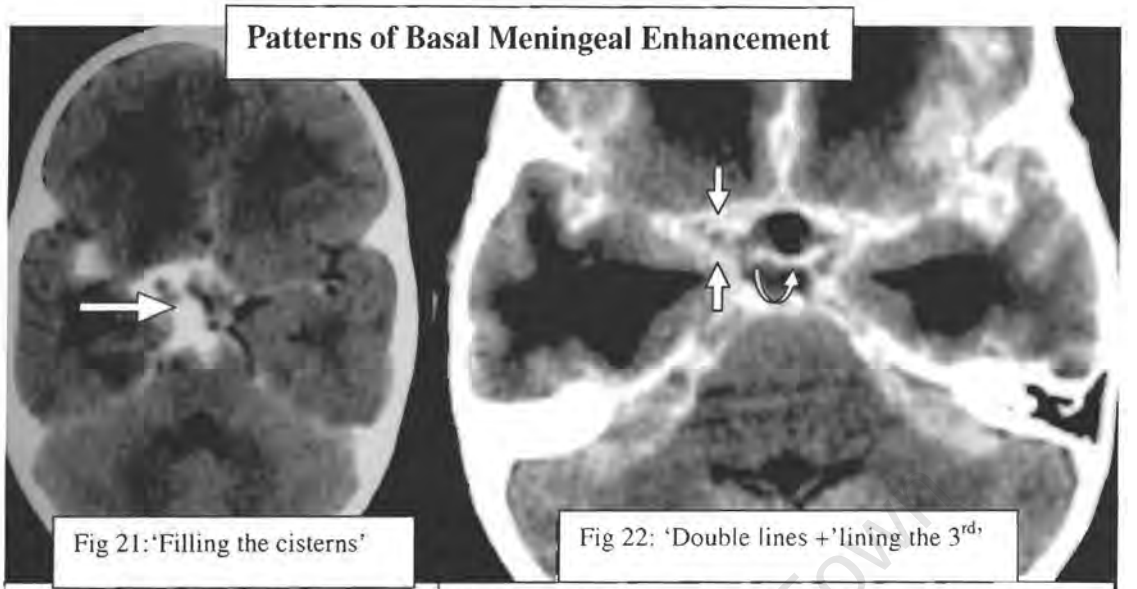

Fig 21: 'Filling the cisterns'

Axial post-contrast CT scan shows asymmetrical enhancement of the suprasellar cistern contents on the right (arrow).

Fig 22: 'Double lines +' lining the 3rd'

Post contrast CT scan shows enhancement of the meninges forming the suprasellar cistern margins. There are 'double lines' in the right middle cerebral artery cistern (arrows), where the enhanced middle cerebral artery lies adjacent to the posterior part of the frontal lobe meninges, which are also enhancing. Note the abnormal enhancement lining the posterior part of the infundibular recess of the dilated third ventricle (curved arrow).

Fig 23: 'Double lines' + 'lining the 3rd'

There is subtle basal meningeal enhancement in this post-contrast CT scan. 'Double lines' are seen in the right middle cerebral artery cistern (arrows) where the abnormally enhancing meninges of the frontal lobe lie adjacent to those of the temporal lobe. Note the abnormal circumferential enhancement associated with the infundibular recess of the third ventricle (curved arrow).

Fig 24: 'Linearity', 'Filling the cisterns' + 'Ill-defined edge'

There is abnormal asymmetrical enhancement of the content of the left middle cerebral artery cistern, seen as a linear band over numerous contiguous CT slices (curved arrow). This has an ill-defined edge and is associated with 'border-zone' infarctions in the left frontal and temporal lobes. The findings are in sharp contrast to those on the right where the normal right middle cerebral artery is not seen as linearity, but is interrupted in appearance due to its tortuous course over contiguous slices (arrows). Both the right middle cerebral artery and the basilar artery show sharp margins and are relatively thin compared to the abnormal left middle cerebral artery cistern enhancement.

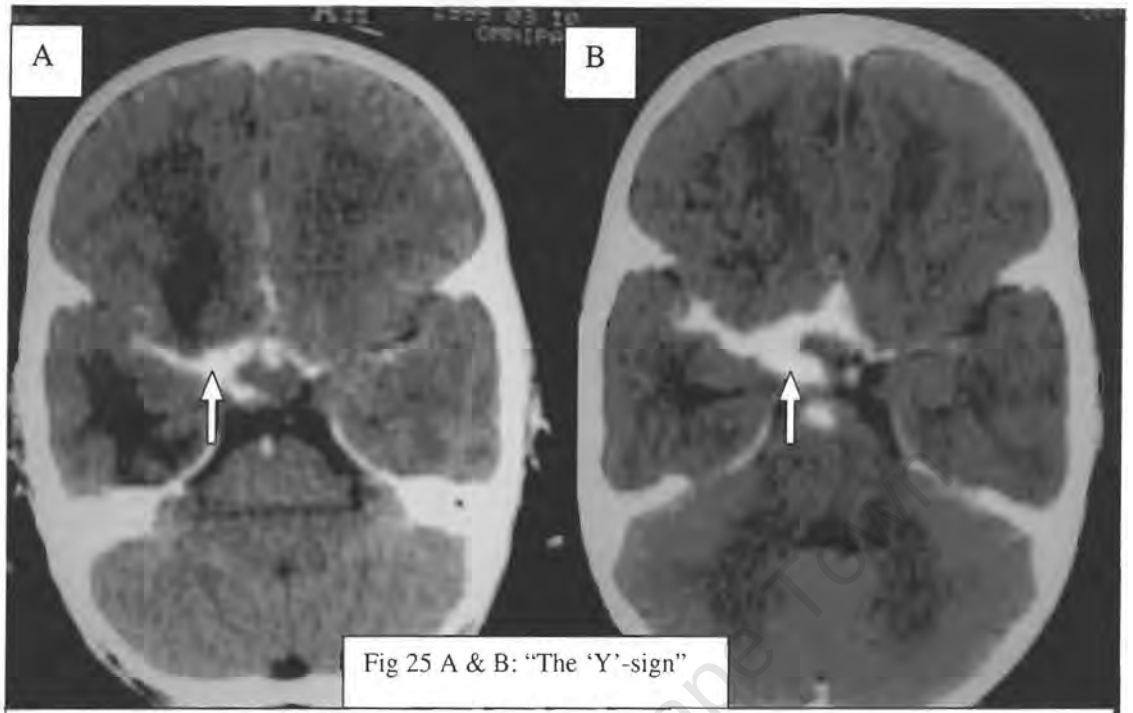

Fig 25 A & B: "The 'Y'-sign"

Two examples showing right middle cerebral cistern enhancement continuous with the suprasellar cistern in the shape of a horizontally oriented 'Y'. This is not seen in normal enhancement of the circle of Willis vessels because the posterior communicating artery is not well enough seen to produce the posteromedial arm of the 'Y', as seen on the right in both cases. Image (A) also shows 'border zone' infarction, not present in the second patient, in whom the meningeal / cisternal enhancement is more exaggerated. In (B) there is associated focal pontine enhancement consistent with nodular enhancement of a tuberculoma.

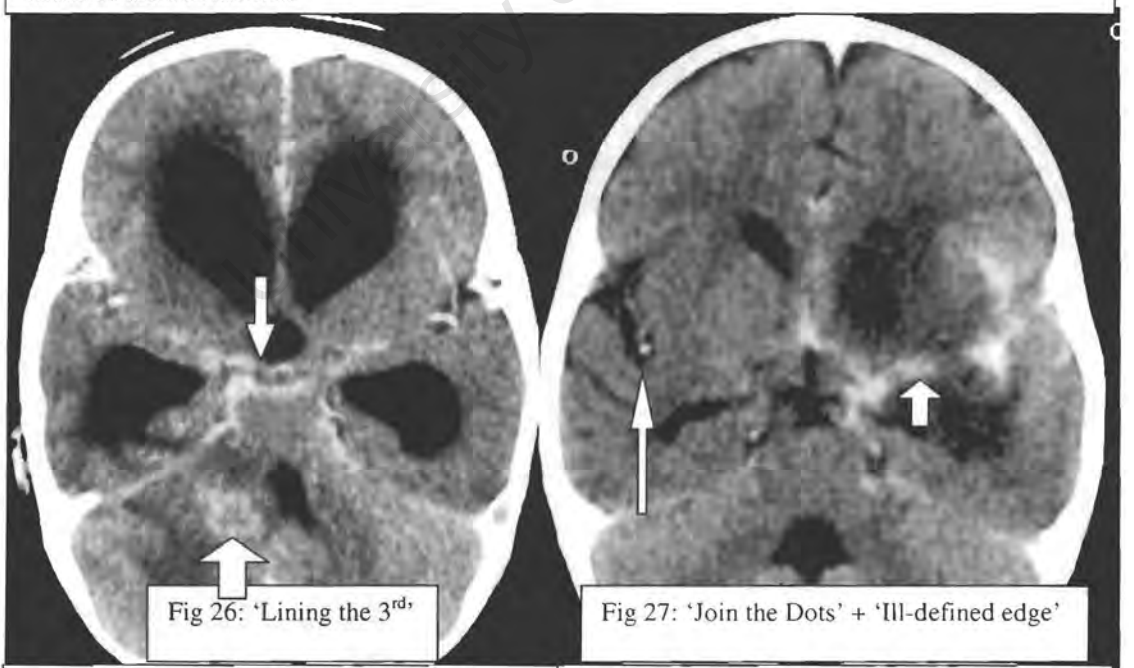

Fig 26: 'Lining the 3rd'

There is subtle abnormal meningeal enhancement lining the posterior aspect of the outer wall of the infundibular recess of the third ventricle (thin arrow). A granuloma is seen in the right cerebellar white matter (short arrow) and there is associated hydrocephalus.

Fig 27: 'Join the Dots' + 'Ill-defined edge'

Abnormal asymmetrical enhancement involving the left side of the suprasellar cistern and left middle cerebral artery cistern, extending to involve the left Sylvian cistern, (short arrow). This is in contrast to the normal separate and sharply marginated right Sylvian branches of the right middle cerebral artery (long arrow). The linear enhancement in the Sylvian fissure has been termed the 'join the dots' sign. Note also the associated left 'border zone' infarcts.

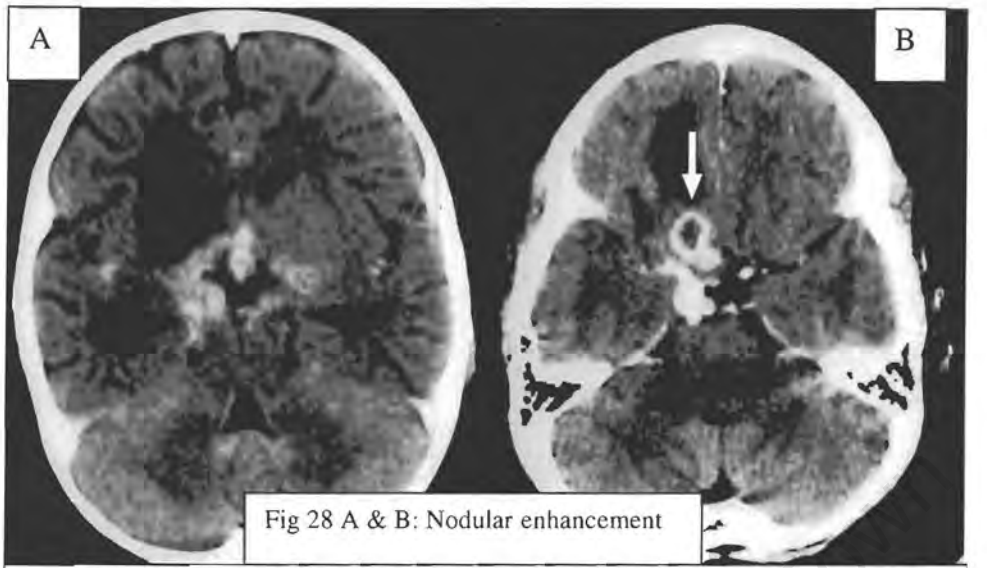

Fig 28 A & B: Nodular enhancement

Both figures show nodular basal meningeal enhancement. In (B) there is ring-enhancement (arrow). Both cases show associated right-sided infarcts, as well as prominent surface markings and ventricles. The latter feature may either be the result of cerebral atrophy, temporary shrinkage or mild communicating hydrocephalus.

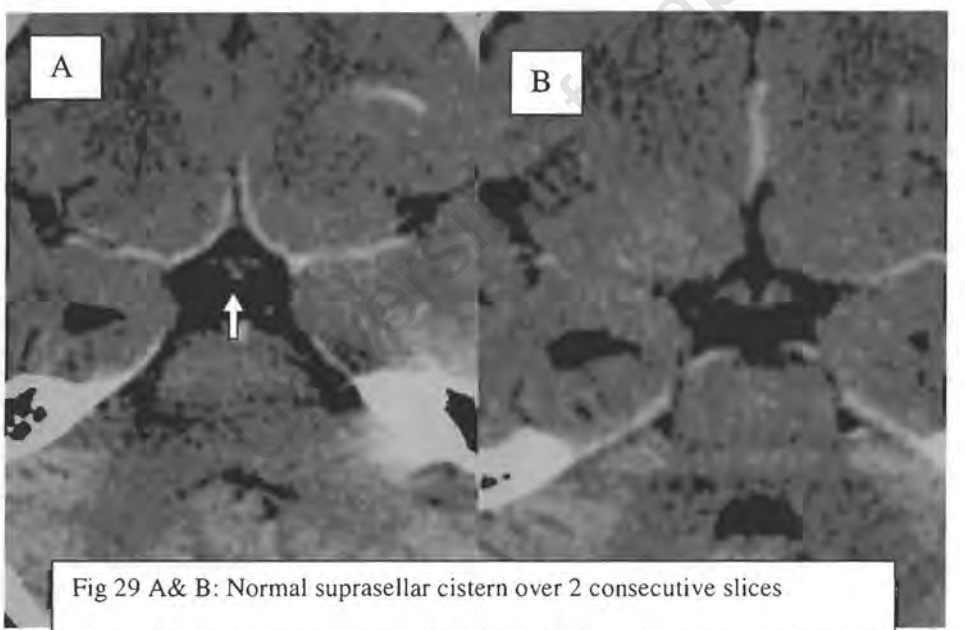

Fig 29 A& B: Normal suprasellar cistern over 2 consecutive slices

An example of the normal suprasellar cistern and enhancement of the circle of Willis vessels. Note the sharply marginated, smooth vessels, absence of 'Y' signs and double lines, no enhancement posterior to the infundibular recess of the third ventricle and no cisternal filling with contrast. If the proximal middle cerebral artery is seen as a linear structure, it should be on one slice only. The distal artery may be seen as a linear structure on more than one slice as this branches near the Sylvian cisterns. Smooth and sharply marginated enhancement of the meningeal covering of the infundibulum is normal (arrow).

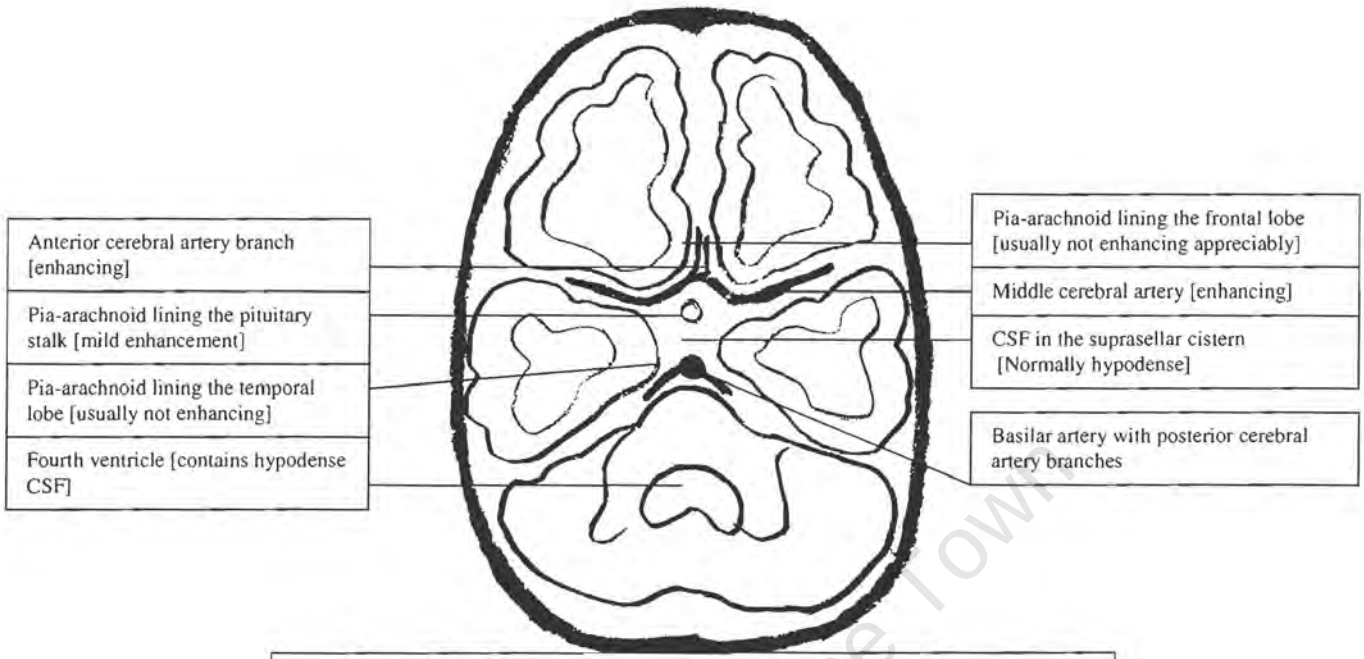

Fig 30: Line diagram demonstrating the normal contents and expected enhancement pattern of the suprasellar cistern and circle of Willis vessels visible on CT.

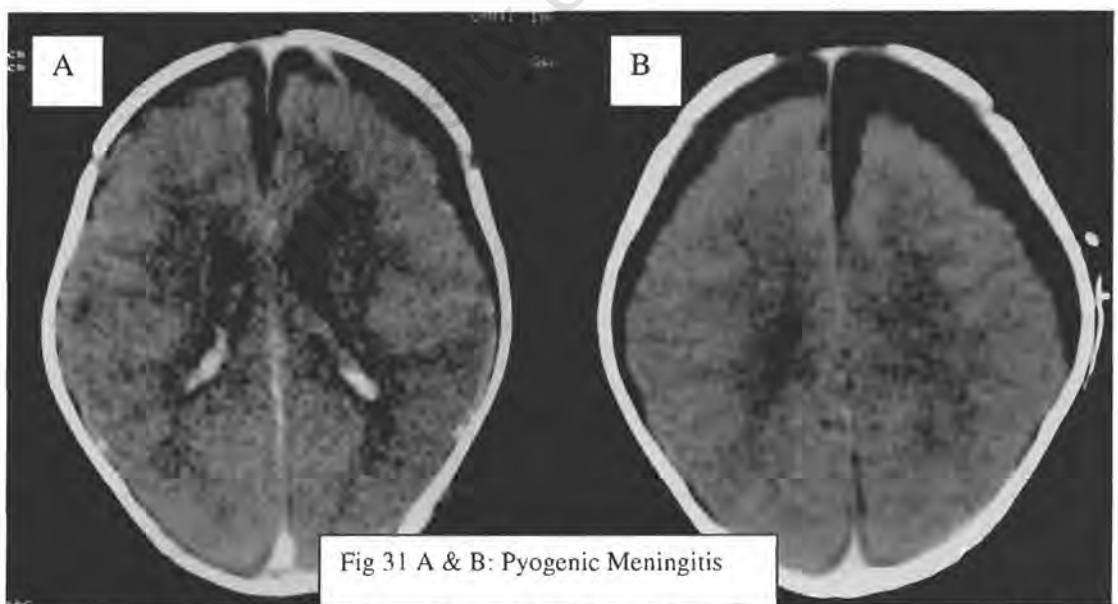

Fig 31 A & B: Pyogenic Meningitis

In comparison to TBM, a patient in the 'Negative' group with pyogenic meningitis shows no features of basal meningeal enhancement but does show mild to moderate hydrocephalus and non-enhancing CSF-density subdural surface effusions, which are a feature of pyogenic meningitis

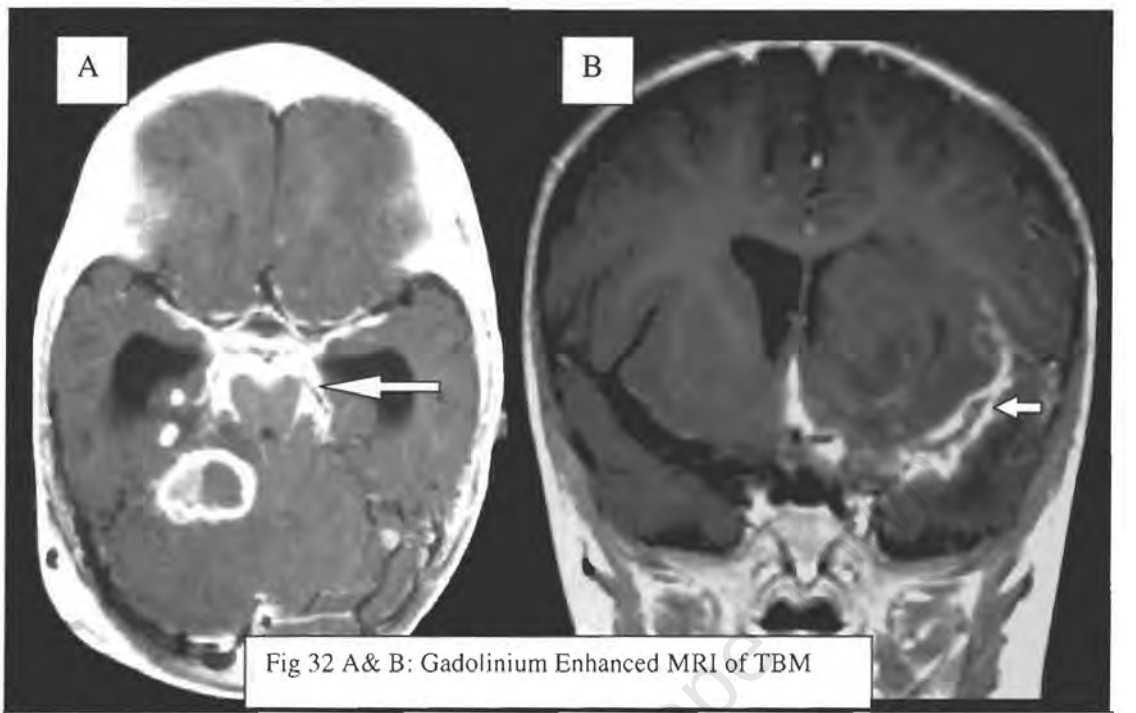

Fig 32 A& B: Gadolinium Enhanced MRI of TBM

MRI scanning shows basal enhancement with greater sensitivity than does CT, as in Fig 32A, which also demonstrates a tuberculoma and hydrocephalus. Note that on MRI vessels usually stand out as hypo-intense 'flow-voids' within the abnormal cisternal enhancement (long arrow). The second image confirms the CT finding of 'double lines' (short arrow) in this patient with asymmetrical enhancement of the suprasellar and left middle cerebral artery cistern.

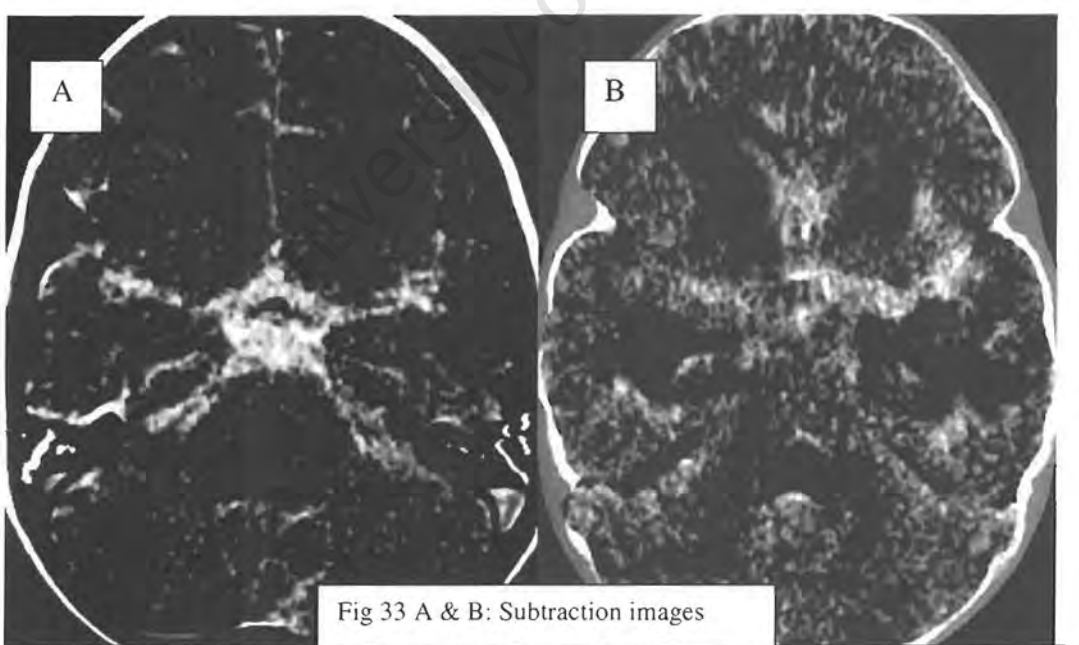

Fig 33 A & B: Subtraction images

Images formed by subtracting the non-contrast from the contrast study demonstrate the basal enhancement even in the presence of hyperdense exudates on the non-contrast study

CT Findings – Hydrocephalus

Hydrocephalus is reported to occur frequently in TBM [11,18,22,32,43], involving between 75 and 100% of paediatric cases [8,11,59]. Numerous authors report that it is the most frequent CT feature of TBM [8,15,27,41-43,50], especially in infants and children [3,42]. This view is not supported by the findings of this thesis. Hydrocephalus is, however, the most treatable complication of TBM [40,43,52,59]. A number of reasons have been advanced in the literature for the observation that hydrocephalus detected on CT may be unreliable diagnostically and prognostically, and less frequent and less significant than previously held. They are tabulated below:

-Hydrocephalus is a **late occurrence** in TBM [10,11,18,32], usually only manifesting 4 to 6 weeks into the disease [11,42]. It may therefore not be present on initial scans.

-Hydrocephalus is **not specific** for TBM, and can follow other infections, including fungal, viral, bacterial and toxoplasma infections, as well as bleeding into the subarachnoid space.

-Communicating hydrocephalus (especially when it is due to impaired CSF absorption) may readily be **confused with atrophy** [22,40,52]. Attempts were made to differentiate the two entities by recording which patients with ventriculomegaly in our series had features inseparable from atrophy (i.e. moderately enlarged ventricles with associated prominence of the surface markings). Atrophy may occur secondary to TBM [52], or from under nourishment, which may be concurrently present in a significant number of patients in the developing world [40].

-Assessment of whether ventriculomegally constitutes hydrocephalus makes use of **subjective parameters** (described by Schoeman and co-workers in 3 different papers) [40,52,59]. The size of the ventricles is classically expressed as the ratio of bifrontal ventricular to biparietal diameters (Evan's ratio) [75,76] and does not allow for parenchymal losses seen in atrophy and TB infection [22,52,40].

-Periventricular lucency is considered to represent transependymal CSF flow or backup in severe hydrocephalus (figure 34 a and b) [34], and has been subjectively graded as mild, moderate or severe [59]. This does not account for the age-related differences in the state of myelin maturation, or other causes of white matter low density, such as oedema

or infarction [59]. This finding also shows no relation to clinical outcome or CSF pressure [40]. One author emphasises that it is an unreliable measure of hydrocephalus [34].

-The size of the **sulcal markings**, which is variable and prominent in infants (figure 35 a and b), is also a subjective measure of hydrocephalus. Widening of sulci occurs with both cerebral atrophy [52,59] and impaired CSF absorption [40].

-The presence of hydrocephalus **does not correlate** with other important parameters such as ventricular or intracranial pressures [40,52,59], the clinical presentation [18], or the outcome [40,52]

-**No associations** have been established between:

(a) Periventricular lucency and raised intracranial pressure

(b) Raised pressure and outcome [52]

c) Late shunting and outcome [40].

-**Differentiation between communicating and non-communicating** hydrocephalus on CT is not possible and does not aid in predicting tonsillar herniation after lumbar puncture [29,40].

Hydrocephalus has been found in this study to be both less sensitive (68%) than basal enhancement, and less specific (72%) than non-contrast density in the diagnosis of TBM (likelihood ratio of 2.4.). There is however a statistically significant difference in the presence of hydrocephalus between the 2 groups of patients (p=0.0016). It is neither a sensitive nor specific CT sign for TBM when compared to basal enhancement and non-contrast density respectively.

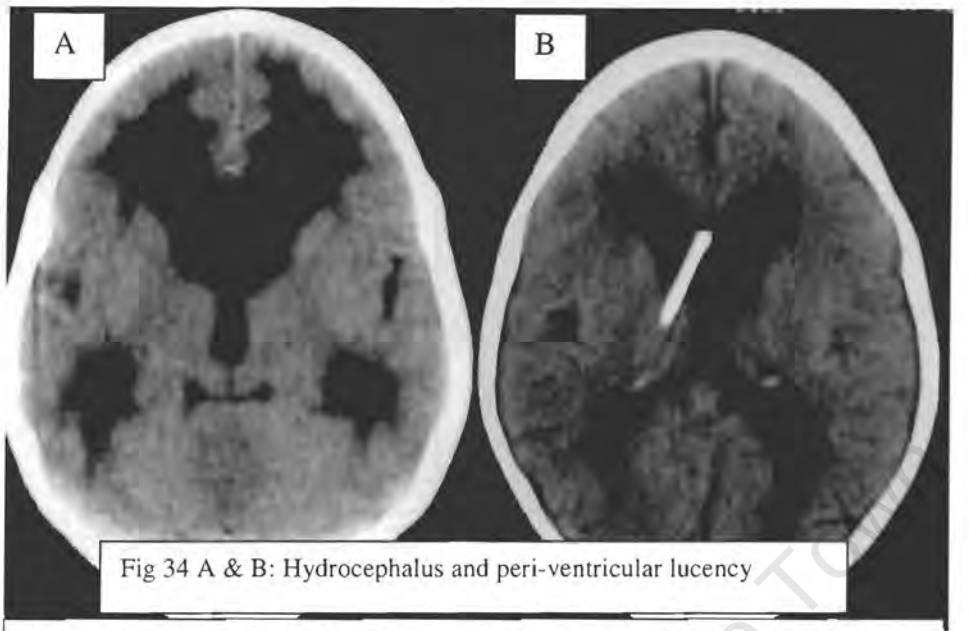

Fig 34 A & B: Hydrocephalus and peri-ventricular lucency

Severe non-communicating hydrocephalus with marked peri-ventricular low density representing transependymal fluid shift (left). After insertion of a ventriculo-peritoneal shunt, the ventricles are decompressed, the surface markings have re-appeared and the peri-ventricular low density has resolved (right).

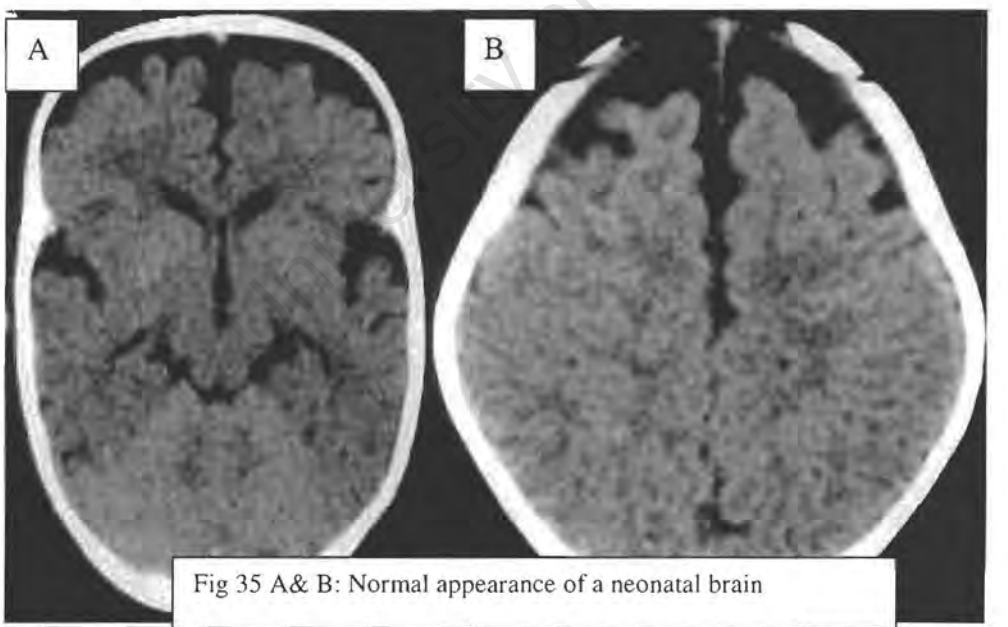

Fig 35 A& B: Normal appearance of a neonatal brain

Patients who are less than a year of age, such as the patient imaged above, have prominent subarachnoid spaces because of physiological immaturity of the arachnoid granulations and poor re-absorption of CSF (a physiological communicating hydrocephalus). This may be inseparable from communicating hydrocephalus due to pathologically impaired re-absorption of CSF; from atrophy due to the TBM or co-existing malnutrition; and from temporary shrinkage due to dehydration.

Table 8: CT results for TBM in children: comparison with published series

Study	Total Patients	Children	Hydro-cephalus	Basal Enhance	Infarcts Parenchymal Destruction	Tuberculoma
Bhargava (1982)[33]	60	36	83%	82%	28%	10%
Upadhyaya (1983)[36]	59(70)	59	100%	No result	6%	8%
Artopoulos (1984)[37]	9	9	100%	11%	44%	56%
Schoeman (1985)[52]	24	24	87%	No result	No result	No result
Kingsley (1987)[32]	25	12	72%	No result	67%	No result
Leiguarda (1988)[39]	65	65	89%	69%	38%	27%
Wacker (1990)[7]	30	30	100%	37%	37%	No result
Altunbasak (1994)[41]	52	52	98%	52%	25%	No result
Schoeman (1995)[40]	198	198	83%	75%	38%	11%
Kumar (1996)[46]	94	94	81%	83%	19%	24%
Patwari (1996)[49]	136	136	32%	No result	13%	27%
Ozates (2000)[18]	289	214	80%	15%	14%	4%
Farinha (2000)[10]	33	33	94%	93%	33%	15%
Kemaloglu (2002)[42]	156	156	No result	46%	22%	4%
Tung (2002)[8]	7	7	100%	14%	29%	No result
De (2002)[71]	21	21	76%	67%	50%	10%
Andronikou (2004)	37	37	68%	89%	62%	13.5%
Average	79	74	84%	56%	33%	18%

['No result' indicates report did not provide that information]

[Averages exclude our patients (Andronikou et al)]

Table 9: CT results of TBM in adults: comparison with published series

Study	Total Patients	Adults	Hydro-cephalus	Basal enhance	Infarcts Parenchymal destruction	Tuberculoma
Bullock (1982)[34]	52	52	76%	64%	32%	No result
Teoh (1989)[28]	64	64	59%	64%	17%	22%
Misra (1996)[6]	64	64	38%	34%	20%	17%
Hosoglu (1998)[4]	64(101)	64	45%	23%	6.3%	12.5%
Kalita (2001)[24]	24	24	67%	38%	50%	13%
Lan (2001)[38]	17	17	82%	41%	47%	12%
Hosoglu (2002)[50]	271(434)	271	47%	8%	14%	8%
Andronikou (2004)	37	0	68%	89%	62%	13.5%
Average	77	77	60%	45%	31%	12%

['No result' indicates the report did not provide that information]

[Numbers in curved brackets are the total numbers studied, numbers outside brackets are those who underwent CT.]

[Averages exclude our numbers (Andronikou et al)]

Other than the study by Farinha et al [10], our series has the highest incidence of basal enhancement and infarcts and the lowest incidence of hydrocephalus of any paediatric series. In comparison to adult series, a significantly higher incidence of basal enhancement and infarcts is present. We presume that this is due to the lack of objective criteria for determining the presence of basal enhancement and because of the possible inclusion of patients with cerebral atrophy into the hydrocephalus group.

Computer Aided Evaluation and Future Applications:

Conversion of the optical densities of digitised images of hard copy films of CT scans to Hounsfield units is not routine practice. The details of this will be available in a Master's thesis that is currently underway. This technique may well be may be useful for other diagnostic work on archived hard-copy film. It permits retrospective measurement of CT density in Hounsfield Units, which is helpful (as in this paper) for retrospective research. Clinically it may offer benefits to patients who migrate to different doctors or countries with hard copies in hand. Modern CT images are frequently transferred electronically or on CD-ROM in Digital Imaging and Communication in Medicine 3 (DICOM 3) format, which allows direct readout of Hounsfield Units.

The method of density thresholding is commercially available on modern CT scanners by simple windowing techniques, and has current uses in eliminating soft tissue or bone from reconstructed CT images or detection of subtle density variations. It has not been previously used (to our knowledge) to demonstrate cisternal hyperdensity. By first determining the highest abnormal density reading using multiple random samplings and then determining the highest normal brain parenchymal density, it is possible to eliminate normal brain parenchyma by setting the lower density threshold value above the highest normal and below the highest abnormal values. An arbitrary upper threshold value was set 4 Hounsfield units above the measured abnormal density reading to eliminate bone from the image.

Once the density elimination was performed by the computer, the remaining image was representative of structures denser than normal brain but less than bone density. One is therefore able to create an image representing a 'cast' of the hyperdensity in the cisterns and confirm the subjective determination of this. In this particular use, the evaluation is convincing because normally the cisterns, especially the basal cisterns, are widely patent in children and contain normal CSF which has the density reading of water (0 HU). This would not contribute to the manipulated image.

Problems of interpretation occur due to 'beam-hardening', a common artefact adjacent to the calvarium and in the posterior fossa. This artefact also becomes more visible on the manipulated image. However, this tends to be present in the periphery and in the posterior fossa, which allows it to be distinguished from the more central location of the basal cisterns.

Other threshold setting applications include use for detection of abnormal basal enhancement. This does somewhat depend on the amount and rate of intravenous contrast enhancement, but has potential in distinguishing pathological from normal basal enhancement in doubtful cases. The computerised semi-automated method can be further modified into a computer aided diagnostic (CAD) system if normal density ranges of parenchyma are entered into a computer programme. This may have uses in the detection of acute subarachnoid blood or other surface haemorrhage that is also hyperdense on non-contrast CT scans.

A method of subtracting the non-contrast images from the post-contrast image has also been attempted. In the case of lack of enhancement, the images would subtract leaving a void, other than the vessels. Any basal enhancement would remain, while the remainder of structures would subtract. A subtracted image in these circumstances may show a typical thick pattern of enhancement different from the normal circle of Willis vessels, which would remain after subtraction. A study to investigate the usefulness of this technique would ideally be performed prospectively as the CT images pre- and post-contrast will have to be identical in position to subtract out appropriately, and in children this may be difficult without sedation.

There may be potential commercial applications for the threshold and computer-aided diagnosis methods described here to reduce the subjective elements of evaluation.

Limitations:

As in any research pertaining to tuberculosis, particularly those affecting children, the low accumulation rate of 'gold standard' diagnosis cases limits the number of patients that can be included. Instead of compromising the 'gold standard' for our research (CSF culture proof) we preferred to perform retrospective research, spanning four years, to obtain an acceptable study group. We were limited to four years, because this covered the period when a new CT scanner was installed and standardized imaging protocols of high standard were commenced (1998). Bayes theorem must be kept in mind as the pre-test likelihood of TBM is high in our community, while other granulomatous meningitides (such as fungal meningitis), which may result in similar CT findings, are rare.

The TBM group in this paper would have consisted of 130 patients had we included the 'Probable' patients (37 'Definite' and 93 'Probable'). In clinical practice the 'Probable' group patients are considered and treated as if they were 'Definite' TBM patients. We have excluded them so as to limit doubt on the accuracy of the CT features. In doing this however, there is a new limitation. A critical observer may suggest that our CT findings may only be positive when there are sufficient organisms to grow in the laboratory. We have therefore also presented the results from the 'Probable' group (that mimic closely the results of the 'Definite' group) but have not included them in our statistical calculations or discussion.

Structuring of a control group was not possible in this study. The 'Negative' group acts as a 'control group', and was designed to represent the true clinical scenario in which patients present with features of meningitis prompting both CSF collection for TB culture and CT scanning to diagnose intracranial pathology. It is possible, however, that cases of TBM with no growth on culture and atypical CSF chemistry have been placed into the 'Negative' group. The clinicians classifying the patients also based the 'Negative' group determination on the culture of an alternative organism, or response to alternative treatment. It has been assumed that in normal subjects the CSF in the supra-sellar cistern is of low density, and that the basal cisterns do not enhance.

Our patient numbers were limited by the unavoidable exclusions that arise when performing retrospective research. The fact that 191 patients had to be excluded from a starting group of 353 because of incomplete records reflects poorly on the organisational structure of the public health system. Thirty-eight patients were excluded because of absent clinical notes, 29 for incomplete clinical notes, 95 for inadequate CSF data and 28 patients for incomplete or inadequate CT studies (10 of who had 'Definite' TBM clinically). Many of these exclusions may not have occurred in prospective research because of standardized data collection, but the patients would still have to meet the criteria of clinically suspected meningitis to be included and qualify for a CT scan. The excluded number of patients does not therefore necessarily imply that the study group would be increased by as many patients had they not been excluded.

We attempted to simulate prospective research by blinding the CT readers to the diagnosis and by randomising the patient's CT scans. We used the reader consensus method because the CT readers varied significantly in experience. We pre-defined objective parameters for the presence of 'basal enhancement' and 'non-contrast density' because these are not clearly defined in the literature, so as to make the assessment more objective. For the new feature of 'non-contrast cisternal density' we also used a digitised method of confirming the results that we recorded as positive to minimize subjectivity, which is an inherent limitation of diagnostic imaging.

With regard to hydrocephalus, we recorded any patient with ventriculomegaly as positive. We also recorded in which patients we could not differentiate it from atrophy but used the former (larger) group for our statistical analysis so as not to undermine the feature being challenged in our aim.

Finally, a major limitation is not having the HIV results of our patients, because as mentioned in the body of our discussion, this could affect the appearances of TBM on CT scanning. This does not make our conclusion invalid or weaker. HIV may result in fewer patients exhibiting basal enhancement (and presumably the 'non-contrast density', as they both represent the exudates) and more patients would be recorded with

hydrocephalus because of the atrophy in HIV, which is the commonest finding. These findings should weaken our results rather than falsely inflating them.

Conclusion:

We have demonstrated that basal enhancement is the most sensitive feature for diagnosing TBM. A patient not showing basal enhancement is unlikely to have TBM; i.e. it is useful for ruling out the disease. Identification of hyperdensity in the basal cisterns prior to contrast administration is the most specific single feature for diagnosing TBM and is most useful for 'ruling in' disease. In practice the strong positive predictive value for the presence of non-contrast hyperdensity in the diagnosis of TBM allows a confident diagnosis to be made when it is identified and saves both resources and time, making a post-contrast study unnecessary. It is however only present in 46% of patients with definite TBM.

Complications of TBM, including hydrocephalus and infarction are also visible on non-contrast CT scanning. Failure to demonstrate hyperdensity in the cisterns on the non-contrast study should prompt the administration of intravenous contrast and repeat CT. Either hydrocephalus or infarction, or both in conjunction with basal enhancement, also allow a confident diagnosis of TBM to be made.

Automated and semi-automated diagnosis of TBM based on our computer software package to identify non-contrast hyperdensity in the basal cisterns is a reality and allows rapid diagnosis without the presence of a radiologist. Objective criteria that are currently being tested may assist in better detection of abnormal basal enhancement and our suggested subtraction method is, we believe, a novel idea for minimizing reader bias. The presence of non-contrast hyperdensity and post-contrast basal enhancement on CT are more specific and more sensitive respectively than is hydrocephalus in childhood TBM, supporting our hypothesis.

References:

1] Starke JR, Jacobs RF, Jereb J. Resurgence of tuberculosis in children. J Pediatr. 1992 Jun;120(6):839-55

2] Buttaro TM, Ezell B, Gray V. A care plan for children with tuberculosis. Public Health Nurs. 1995 Jun;12(3):181-8

3] de Castro CC, de Barros NG, Campos ZM, Cerri GG. CT scans of cranial tuberculosis. Radiol Clin North Am. 1995 Jul;33(4):753-69

4] Hosoglu S, Ayaz C, Geyik MF, Kokoglu OF, Ceviz A. Tuberculous meningitis in adults: an eleven-year review. Int J Tuberc Lung Dis. 1998 Jul;2(7):553-7

5] Katrak SM, Shembalkar PK, Bijwe SR, Bhandarkar LD. The clinical, radiological and pathological profile of tuberculous meningitis in patients with and without human immunodeficiency virus infection. J Neurol Sci. 2000 Dec 1;181(1-2):118-26

6] Misra UK, Kalita J, Srivastava M, Mandal SK. Prognosis of tuberculous meningitis: a multivariate analysis. J Neurol Sci. 1996 Apr;137(1):57-61

7] Waecker NJ Jr, Connor JD. Central nervous system tuberculosis in children: a review of 30 cases. Pediatr Infect Dis J. 1990 Aug;9(8):539-43

8] Tung YR, Lai MC, Lui CC, Tsai KL, Huang LT, Chang YC, Huang SC, Yang SN,Hung PL. Tuberculous meningitis in infancy. Pediatr Neurol. 2002 Oct;27(4):262-6

9] Kumar R, Singh SN, Kohli N. A diagnostic rule for tuberculous meningitis. Arch Dis Child. 1999 Sep;81(3):221-4

10] Farinha NJ, Razali KA, Holzel H, Morgan G, Novelli VM. Tuberculosis of the central nervous system in children: a 20-year survey. J Infect. 2000 Jul;41(1):61-8

11] Lamprecht D, Schoeman J, Donald P, Hartzenberg H. Ventriculoperitoneal shunting in childhood tuberculous meningitis. Br J Neurosurg. 2001 Apr;15(2):119-25

12] Kochi A. The global tuberculosis situation and the new control strategy of the World Health Organization. Tubercle. 1991 Mar;72(1):1-6.

13] Schutte CM. Clinical, cerebrospinal fluid and pathological findings and outcomes in HIV-positive and HIV-negative patients with tuberculous meningitis. Infection. 2001 Aug;29(4):213-7.

14] Beskonakli E, Cayli S, Turgut M, Yalcinlar Y. Primary giant granulomatous basal meningitis: an unusual presentation of tuberculosis. Childs Nerv Syst. 1998 Jan-Feb;14(1-2):79-81

15] Clark WC, Metcalf JC Jr, Muhlbauer MS, Dohan FC Jr, Robertson JH. Mycobacterium tuberculosis meningitis: a report of twelve cases and a literature review. Neurosurgery. 1986 May;18(5):604-10.

16] Cassleman ES, Hasso AN, Ashwal S, Schneider S. Computed tomography of tuberculous meningitis in infants and children. J Comput Assist Tomogr. 1980 Apr;4(2):211-6

17] Hooijboer PG, van der Vliet AM, Sinnige LG. Tuberculous meningitis in native Dutch children: a report of four cases. Pediatr Radiol. 1996;26(8):542-6

18] Ozates M, Kemaloglu S, Gurkan F, Ozkan U, Hosoglu S, Simsek MM. CT of the brain in tuberculous meningitis. A review of 289 patients. Acta Radiol. 2000 Jan;41(1):13-7

19] Price HI, Danziger A. Computed tomography in cranial tuberculosis. AJR Am J Roentgenol. 1978 Apr;130(4):769-71

20] Donald PR, Cotton MF, Hendricks MK, Schaaf HS, DE Villiers JN, Willemse TE. Pediatric meningitis in the Western Cape Province of South Africa. Journal of Tropical Pediatrics. 1996;42: 256-61

21] Leonard JM, Des Prez RM. Tuberculous meningitis. Infect Dis Clin North Am. 1990 Dec;4(4):769-87

22] Trautmann M, Kluge W, Otto HS, Loddenkemper R. Computed tomography in CNS tuberculosis. Eur Neurol. 1986;25(2):91-7

23] Berenguer J, Moreno S, Laguna F, Vicente T, Adrados M, Ortega A, Gonzalez-LaHoz J, Bouza E. Tuberculous meningitis in patients infected with the human immunodeficiency virus. N Engl J Med. 1992 Mar;326(10):668-72

24] Kalita J, Misra UK. Brainstem auditory evoked potentials in tubercular meningitis and their correlation with radiological findings. Neurol India. 2001 Mar;49(1):51-4

25] Smith MH. Tuberculosis in children and adolescents. Clin Chest Med. 1989 Sep;10(3):381-95

26] Rovira M, Romero F, Torrent O, Ibarra B (1980) Study of Tuberculous Meningitis by CT. Neuroradiology 19:137-141

27] Witrak BJ, Ellis GT. Intracranial tuberculosis: manifestations on computerized tomography. South Med J. 1985 Apr;78(4):386-92

28] Teoh R, Humphries MJ, Hoare RD, O'Mahony G. Clinical correlation of CT changes in 64 Chinese patients with tuberculous meningitis. J Neurol. 1989 Jan;236(1):48-51

29] Schoeman JF, Van Zyl LE, Laubscher JA, Donald PR. Effect of corticosteroids on intracranial pressure, computed tomographic findings, and clinical outcome in young children with tuberculous meningitis. Pediatrics. 1997 Feb;99(2):226-31

30] Chang KH, Han MH, Roh JK, Kim IO, Han MC, Choi KS, Kim CW. Gd-DTPA enhanced MR imaging in intracranial tuberculosis. Neuroradiology. 1990;32(1):19-25

31] Cho IC, Chang KH, Kim YH, Kim SH, Yu IK, Han MH. MRI features of choroid plexitis. Neuroradiology. 1998 May;40(5):303-7

32] Kingsley DP, Hendrickse WA, Kendall BE, Swash M, Singh V. Tuberculous meningitis: role of CT in management and prognosis. J Neurol Neurosurg Psychiatry. 1987 Jan;50(1):30-6

33] Bhargava S, Gupta AK, Tandon PN. Tuberculous meningitis--a CT study. Br J Radiol. 1982 Mar;55(651):189-96

34] Bullock MR, Welchman JM. Diagnostic and prognostic features of tuberculous meningitis on CT scanning. J Neurol Neurosurg Psychiatry. 1982 Dec;45(12):1098-101

35] Dastur DK. Neurosurgically relevant aspects of pathology and pathogenesis of intracranial and intraspinal tuberculosis. Neurosurg Rev. 1983;6(3):103-10

36] Upadhyaya P, Bhargava S, Sundaram KR, Mitra DK, George J, Singh DC. Hydrocephalus caused by tuberculous meningitis: clinical picture, CT findings and results of shunt surgery. Z Kinderchir. 1983 Dec;38 Suppl 2:76-9

37] Artopoulos J, Chalemis Z, Christopoulos S, Manios S, Kelekis L. Sequential computed tomography in tuberculous meningitis in infants and children. Comput Radiol. 1984 Sep-Oct;8(5):271-7

38] Lan SH, Chang WN, Lu CH, Lui CC, Chang HW. Cerebral infarction in chronic meningitis: a comparison of tuberculous meningitis and cryptococcal meningitis. QJM. 2001 May;94(5):247-53

39] Leiguarda R, Berthier M, Starkstein S, Nogues M, Lylyk P. Ischemic infarction in 25 children with tuberculous meningitis. Stroke. 1988 Feb;19(2):200-4

40] Schoeman JF, Van Zyl LE, Laubscher JA, Donald PR. Serial CT scanning in childhood tuberculous meningitis: prognostic features in 198 cases. J Child Neurol. 1995 Jul;10(4):320-9

41] Altunbasak S, Alhan E, Baytok V, Aksaray N, Yuksel B, Onenli N. Tuberculous meningitis in children. Acta Paediatr Jpn. 1994 Oct;36(5):480-4

42] Kemaloglu S, Ozkan U, Bukte Y, Ceviz A, Ozates M. Timing of shunt surgery in childhood tuberculous meningitis with hydrocephalus. Pediatr Neurosurg. 2002 Oct;37(4):194-8

43] Gelabert M, Castro-Gago M. Hydrocephalus and tuberculous meningitis in children. Report on 26 cases. Childs Nerv Syst. 1988 Oct;4(5):268-70

44] Khan IM, Khan S, Laaser U. Tuberculous meningitis: a disease of fatal outcome in children. Eur J Pediatr. 2003 Apr;162(4):281-2.

45] Ahuja GK, Mohan KK, Prasad K, Behari M. Diagnostic criteria for tuberculous meningitis and their validation. Tuber Lung Dis. 1994 Apr;75(2):149-52

46] Kumar R, Kohli N, Thavnani H, Kumar A, Sharma B. Value of CT scan in the diagnosis of meningitis. Indian Pediatr. 1996 Jun;33(6):465-8

47] Schoeman J, Hewlett R, Donald P. MR of childhood tuberculous meningitis. Neuroradiology. 1988;30(6):473-7

48] Trautmann M, Lindner O, Haase C, Bruckner O. Focal tuberculous meningoencephalitis. Eur Neurol. 1983;22(6):417-20

49] Patwari AK, Aneja S, Ravi RN, Singhal PK, Arora SK. Convulsions in tuberculous meningitis. J Trop Pediatr. 1996 Apr;42(2):91-7

50] Hosoglu S, Geyik MF, Balik I, Aygen B, Erol S, Aygencel TG, Mert A, Saltoglu N, Dokmetas I, Felek S, Sunbul M, Irmak H, Aydin K, Kokoglu OF, Ucmak H, Altindis M, Loeb M. Predictors of outcome in patients with tuberculous meningitis. Int J Tuberc Lung Dis. 2002 Jan;6(1):64-70.

51] Berti LC. Childhood tuberculosis. J Pediatr Health Care. 1996 May-Jun;10(3):106-14

52] Schoeman JF, le Roux D, Bezuidenhout PB, Donald PR. Intracranial pressure monitoring in tuberculous meningitis: clinical and computerized tomographic correlation. Dev Med Child Neurol. 1985 Oct;27(5):644-54

53] Ravenscroft A, Schoeman JF, Donald PR. Tuberculous granulomas in childhood tuberculous meningitis: radiological features and course. J Trop Pediatr. 2001 Feb;47(1):5-12

54] Moodley M, Bamber S. The operculum syndrome: an unusual complication of tuberculous meningitis. Dev Med Child Neurol. 1990 Oct;32(10):919-22

55] Murray SJ, Barret A, Magee JG, Freeman R. Optimisation of acid fast smears for the direct detection of mycobacteria in clinical samples. J Clin Pathol. 2003 Aug;56(8):613-5

56] Doucet-Populaire F, Lalande V, Carpentier E, Bourgoin A, Dailloux M, Bollet C, Vachee A, Moinard D, Texier-Maugein J, Carbonnelle B, Grosset J. A blind study of the polymerase chain reaction for the detection of Mycobacterium tuberculosis DNA. Azay Mycobacteria Study Group. Tuber Lung Dis. 1996 Aug;77(4):358-62

57] Lodha R, Kabra SK. Newer diagnostic modalities for tuberculosis. Indian J Pediatr. 2004 Mar;71(3):221-7

58] Perkins MD, Conde MB, martins M, Kritski AL. serologic diagnosis of tuberculosis using a simple commercial multiantigen assay. Chest. 2003 Jan;123(1):107-12

59] Schoeman JF, Laubscher JA, Donald PR. Serial lumbar CSF pressure measurements and cranial computed tomographic findings in childhood tuberculous meningitits. Childs Nerv Syst. 2000 Apr;16(4):203-8; discussion 209

60] Daoud AS, Omari H, al-Sheyyab M, Abuekteish F. Indications and benefits of computed tomography in childhood bacterial meningitis. J Trop Pediatr. 1998 Jun;44(3):167-9

61] Gilman S. Imaging the brain. First of two parts. N Engl J Med. 1998 Mar 19;338(12):812-20

62] Oldendorf WH. The quest for an image of brain: a brief historical and technical review of brain imaging techniques. Neurology. 1978 Jun;28(6):517-33

63] Harwood-Nash D, Grossman H, Felman A, Kirkpatrick J, Swischuk L. American Academy of Pediatrics Committee on Radiology: Computerized tomography: a perspective in the pediatric patient. Pediatrics. 1977 Feb;59(2):305-8

64] Harwood-Nash DC, Fitz CR, Reilly BJ. Cranial computed tomography in infants and children. Can Med Assoc J. 1975 Sep 20;113(6):546-9

65] Elke M. One century of diagnostic imaging in medicine. Experientia. 1995 Jul 14;51(7):665-80

66] New PF, Scott WR, Schnur JA, Davis KR, Taveras JM. Computerized axial tomography with the EMI scanner. Radiology. 1974 Jan;110(1):109-23

67] Houser O, Smith JB, Gomez MR, Baker HL. Evaluation of intracranial disorders in children by computerized transaxial tomography: a preliminary report. Neurology. 1975 Jul;25(7):607-13

68] Hounsfield GN. Computerized transverse axial scanning (tomography). 1. Description of system. Br J Radiol. 1973 Dec;46(552):1016-22

69] Baker HL Jr, Campbell JK, Houser OW, Reese DF, Sheedy PF, Holman CB. Computer assisted tomography of the head. An early evaluation. Mayo Clin Proc. 1974 Jan;49(1):17-27

70] Gado MH, Phelps ME, Coleman RE. An extravascular component of contrast enhancement in cranial computed tomography. Part I. The tissue-blood ratio of contrast enhancement. Radiology. 1975 Dec;117(3 Pt 1):589-93

71] De JK, Bagchi S, Bhadra UK, Chatterjee SN, Munshi AK. Computerised tomographic study of tuberculous meningitis in children.
J Indian Med Assoc. 2002 Oct;100(10):603-4, 606. Erratum in: J Indian Med Assoc. 2002 Nov;100(11):678.

72] Offenbacher H, Fazekas F, Schmidt R, Kleinert R, Payer F, Kleinert G, Lechner H. MRI in tuberculous meningoencephalitis: report of four cases and review of the neuroimaging literature. J Neurol. 1991 Sep;236(6):340-4

73] [No authors listed] Neuroradiology case of the day. Meningitis caused by Neisseria meningitidis. AJR Am J Roentgenol. 1992 Jun;158(6):1380-1

74] Jinkins JR. Dynamic CT of tuberculous meningeal reactions. Neuroradiology. 1987;29(4):343-7.

75] O'Hayon BB, Drake JM, Ossip MG, Tuli S, Clarke M. Frontal and occipital horn ratio: A linear estimate of ventricular size for multiple imaging modalities in pediatric hydrocephalus. Pediatr Neurosurg. 1998 Nov;29(5):245-9.

76] Jamous M, Sood S, Kumar R, Ham S. Frontal and occipital horn width ratio for the evaluation of small and asymmetrical ventricles. Pediatr Neurosurg. 2003 Jul;39(1):17-21.

Publications, Presentations, Theses and Further Research Resulting from this Project:

Published:

1] Andronikou s, Smith B, Hatherill M, Douis H, Wilmshurst J. Definitive neuroradiological features of tuberculous meningitis in children. Pediatr Radiol. 2004 November;34(11):876-85

2] Andronikou S, Wieselthaler N. Modern imaging of tuberculosis in children: thoracic, central nervous system and abdominal tuberculosis. Pediatr Radiol. 2004 November;34(11):861-75

3] Andronikou S, Wieselthaler N, Smith B, Van Toorn R, Douis H, Fieggen AG, Wilmshurst J. Value of follow-up CT in paediatric tuberculous meningitis. Pediatric Radiology online- DOI: 10.1007/s00247-005-1549-9

Theses:

1] Masters thesis, University of Stellenbosch 2004/5: Przybojewski SJ. (Supervisor: S. Andronikou). Objective criteria to determine the presence of abnormal meningovascular enhancement in children with suspected tuberculous meningitis (TBM)-a computed tomography (CT) study.

2] Masters thesis, UCT 2004/5: Halberstadt W. Pattern recognition in the detection of tuberculous meningitis.

Presentations:

1] Andronikou S. CT scanning in the diagnosis of paediatric TBM: identification of sensitive and objective imaging features. European Society of Pediatric Radiology, Bergen, Norway, 17-21 June 2002.

2] Przybojewski SJ, Andronikou S. Objective criteria to determine the presence of abnormal meningovascular enhancement in children with suspected tuberculous meningitis (TBM)-a computed tomography (CT) study. European Society of Pediatric Radiology, Dublin, Ireland 27 May – 3 June 2005.

Research in Progress:

1] Andronikou S, Wieselthaler N. Infarct distribution in paediatric TBM and correlation with outcome.

List of Tables, Diagrams and Images:

Tables:

Diagrams:

Images:

Grants:

This research was supported by a grant from the Medical Research Council of South Africa.

Acknowledgements:

-My supervisor Steve Beningfield for his unwavering patience, support and wisdom.
-The CT scanner staff at Red Cross Children's Hospital, Jesse Bertelsmann, Dawn Skippers, Cathy Clement, and sister Barbara Duminiet who do not know the word 'no' and pulled and filed more films for me than anyone in the history of the hospital.
-My radiology colleagues, Bruce Smith and Hassan Douis, who patiently reviewed images with me and advised me throughout.
-My clinical colleagues, Jo Wilmshurst and Ronald van Toorn who had to endure repetition of results and constant requests to add more patients.
-Prof. Richard Hewlett for his unique, in-depth insight into the pathology of TBM.
-Mark Hatherill and Lee Liknaitzky/Cullingworth for the statistical analysis.
-Christos Christodoulou for reviewing and editing the manuscript.
-My father Andreas, my mother Andreoula and the remainder of my immediate family for their support.
-Michael Elias, Angelo Fotiadis and Diogo Peral, who regularly stand in as family.

Declaration:

I, Dr. Savvas Andronikou, declare that the work contained within this thesis represents my own work both in concept and design. I acknowledge the assistance of my clinical colleagues Jo Wilmshurst and Ronald Van Toorn for reviewing the patient clinical data and laboratory results, my radiology colleagues Bruce Smith and Hassan Douis who read the CT scans with me as part of a panel, the help of Prof. Richard Hewlett in writing and understanding the pathology component and the assistance of Mark Hatherill and Lee Cullingworth with the statistical analysis.